CT Angiography of Peripheral Arterial Disease

Dominik Fleischmann, MD, Richard L. Hallett, MD, and Geoffrey D. Rubin, MD

Lower-extremity computed tomographic (CT) angiography (ie, peripheral CT angiography) is increasingly used to evaluate patients with peripheral arterial disease. It is therefore increasingly important for all vascular specialists to become familiar with the strengths and limitations of this new technique. The aims of this review are to explain the principles of scanning and injection technique for a wide range of CT scanners, to explain and illustrate the properties of current image postprocessing tools for effective visualization and treatment planning, and to provide an overview of current clinical applications of peripheral CT angiography.

J Vasc Interv Radiol 2006; 17:3–26

Abbreviations: CPR = curved planar reformation, DSA = digital subtraction angiography, MIP = maximum intensity projection, MPR = multiplanar reformation, 3D = three-dimensional, VR = volume reconstruction

ALTHOUGH computed tomographic (CT) imaging of lower-extremity arteries has been attempted with single–detector row scanners (1–5), it was not before the introduction of multiple–detector row CT that adequate resolution imaging of the entire inflow and runoff vessels became possible with a single acquisition and a single intravenous contrast medium injection (6). With increasing availability of multiple–detector row CT scanners, peripheral CT angiography has gradually entered clinical practice (7–11), and as a result of the concomitant rapid evolution of CT scanner technology, high-resolution imaging of the peripheral vasculature has become routinely possible.

For the vascular and interventional radiologist, but also for the vascular surgeon and cardiovascular specialist, it is increasingly important to be familiar with this latest vascular imaging technique, to know its strengths and limitations, and, most importantly, to learn how to read and interpret the large CT angiographic data sets and their reformatted images for clinical decision making and treatment planning.

The organization of this review reflects three interrelated objectives. First, we describe the technical principles of image acquisition and contrast medium injection parameters for a wide range of currently available multiple–detector row CT systems. The level of detail should allow the diagnostic imager to develop his or her own scanner-specific peripheral CT angiography acquisition and injection protocol. Next, we will review the properties of different visualization techniques for extracting the relevant findings and explain how they are interpreted. Finally, we will discuss the accuracy and the practical application of CT angiography within the context of various clinical situations.

SCANNING TECHNIQUE

Peripheral CT angiograms can be obtained with all current multiple–detector row CT scanners (ie, four or more channels). No special hardware is required. With a standardized scanning protocol programmed into the scanner, peripheral CT angiography is a very robust technique for elective and emergency situations. When patients are mobile, the study can easily be performed in 10–15 minutes of room time.

In general, peripheral CT angiography acquisition parameters follow those of abdominal CT angiography. Unless automated tube current modulation is available, a tube voltage of 120 kV and a maximum tube amperage of 300 mA (depending on the scanner) is used for peripheral CT angiography, which results in a similar radiation exposure and dose (12.97 mGy, 9.3 mSv) as abdominal CT angiography (7). Breath-holding is required only at the begining of the CT acquisition through the abdomen and pelvis. Lower amperage (and/or voltage) can and should be used in patients with low body mass index. In obese patients, tube voltage and tube current often need to be increased. A medium to small imaging field of view (with the greater trochanter used as a bony landmark) and a medium to soft reconstruction kernel are generally used for image reconstruction.

SCANNING PROTOCOL

One or more dedicated peripheral CT angiographic acquisition and contrast medium injection protocol(s)

From the Cardiovascular Imaging Section, Department of Radiology, Stanford University Medical Center, 300 Pasteur Drive, S-072, Stanford, California 94305-5105 (D.F., R.L.H., G.D.R.); and Department of Angiography and Interventional Radiology, Medical University of Vienna, Waehringer Guertel 18-20, A-1090, Vienna, Austria (D.F.). Received July 27, 2005; accepted October 8. **Address correspondence to** D.F.; E-mail: d.fleischmann@stanford.edu

None of the authors have identified a conflict of interest.

DOI: 10.1097/01.RVI.0000191361.02857.DE

should be established for each scanner and programmed into the scanner. A full scanning protocol consists of (i) the digital radiograph ("scout" image or "topogram"), (ii) an optional nonenhanced acquisition, (iii) one series for a test bolus or bolus triggering, (iv) the actual CT angiography acquisition series, and (v) a second optional "late-phase" CT angiography acquisition (initiated only on demand) in the event of nonopacification of distal vessels (**Fig 1**).

Patient Positioning and Scanning Range

The patient is placed feet-first and supine on the couch of the scanner. To keep the image reconstruction field of view small, and also to avoid off-center stair-step artifacts (12), it is important to carefully align the patient's legs and feet close to the isocenter of the scanner. Tape may be required to hold a patient's knees together. Although cushions can be used to stabilize the extremities for the patient's comfort, large cushions under the knees should not be used so the field of view can be kept small. Also, as in conventional angiography, excessive plantar flexion of the feet is avoided to prevent an artifactual stenosis or occlusion of the dorsalis pedis artery (ie, "ballerina sign" [13]).

The anatomic coverage extends from the T12 vertebral body level (to include the renal artery origins) proximally through the patient's feet distally (**Fig 1**). The average scan length is between 110 cm and 130 cm. Smaller scan ranges or a smaller field of view (ie, one leg only) may be selected in specific clinical situations.

Image Acquisition and Reconstruction Parameters

The choice of acquisition parameters (ie, detector configuration/pitch) and the corresponding reconstruction parameters (ie, section thickness/reconstruction interval) depends largely on the type and model of the scanner. **Table 1** provides an overview of peripheral CT angiography acquisition parameters for a wide range of multiple–detector row CT scanners, and reflects our clinical experience with four-, 16-, and 64- channel Siemens CT scanners (Siemens, Erlangen, Germany), and four-, eight,- and 16-channel General Electric CT scanners (GE Medical Systems, Milwaukee, WI). Detector configuration is denoted as number of channels times channel width (eg, 4 × 2.5 mm); section thickness and reconstruction interval are expressed as a ratio, eg, 3 mm/1.5 mm.

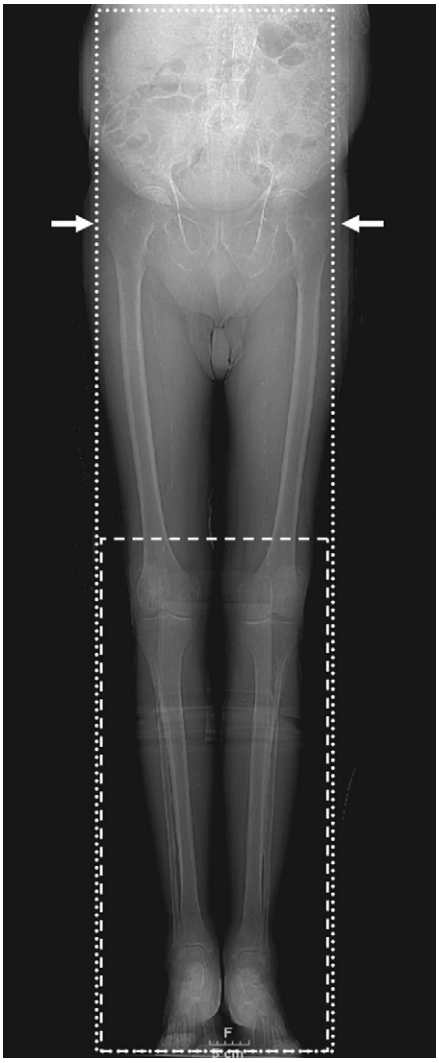

Figure 1. Digital CT radiograph for prescribing peripheral CT angiography. The patient's legs and feet are aligned with the long axis of the scanner. Scanning range (from T12 through the feet) and reconstruction field of view (determined by the greater trochanters; arrows) are indicated by the dotted line. A second optional CT angiography acquisition is prescribed for the crural/pedal territory (dashed line).

Four-channel CT

To cover the entire peripheral arterial tree within acceptable scanning times, the detector configuration is usually set to 4 × 2.5 mm. As a result, the thinnest effective section thickness achievable with these scanners is approximately 3 mm. With overlapping image reconstruction every 1–2 mm, these "standard-resolution" data sets are adequate for visualizing the aortoiliac and femoropopliteal vessels, and also provide enough detail to assess the patency of crural and pedal arteries if vessel calcification is absent or minimal. Four-channel CT therefore provides adequate imaging in patients with intermittent claudication, in acute embolic disease (**Fig 2**), aneurysms, anatomic vascular mapping, and also in the setting of trauma. Such standard-resolution data sets may not be fully diagnostic when visualization of small arterial branches (ie, crural or pedal) is clinically relevant, such as in patients with critical limb ischemia and predominantly distal disease, notably in the presence of excessive arterial wall calcifications. If higher resolution imaging is required and if the clinical situation permits a smaller anatomic coverage area (eg, limited to the legs or to popliteal to pedal vessels only) exquisite high-resolution imaging can also be achieved with four-channel systems with 4 × 1-mm or 4 × 1.25-mm detector collimation (7) within acceptable acquisition times.

Eight-channel CT

A detector configuration of 8 × 1.25 mm permits anatomic coverage of the entire peripheral arterial tree within the same scan time as a 4 × 2.5-mm four-channel CT acquisition at substantially improved resolution. Images with a nominal section thickness of 1.25 mm, reconstructed at 0.8 mm (ie, high resolution) can routinely be acquired. Crural and even pedal arteries can be reliably identified with use of these settings. With faster gantry rotation speed (0.5 sec/360° rotation) and maximum pitch, eight-channel CT allows for extended volume coverage, such as to visualize the entire thoracic, abdominal, and lower-extremity arteries within a single acquisition (**Fig 3**).

Sixteen-channel CT

When a detector configuration of 16 × 1.25 mm or 16 × 1.5 mm is used, similar high-resolution data sets of the

Table 1
CT Acquisition Parameters for Peripheral CT Angiography

Equipment	Gantry Rotation Time (sec)	Detector Configuration (channels × mm)	Pitch	Table Increment (mm/360°)	Table Speed (mm/sec)	Scan Time (sec)†	Injection Protocol (Type)
Four channels							
GE	0.8	4 × 2.5	1.5	15	19	69	Slow
Siemens	0.5	4 × 2.5	1.5	15	30	43	Slow
Eight channels							
GE	0.5	8 × 1.25	1.35	13.5	27	48	Slow
GE	0.5	8 × 2.5	1.35	27	54	24	Fast
Sixteen channels							
GE	0.6	16 × 1.25	1.375	35	46	28	Fast
Siemens	0.5	16 × 1.5	1.2	33	58	23	Fast
Submillimeter							
GE	0.5	16 × 0.625	1.375	17.5	28	47	Slow
Siemens	0.5	16 × 0.75	1.2	18	29	45	Slow
Sixty-four channels							
Siemens	0.5	64 × 0.6‡	0.85	17	32	40	Slow§
Siemens	0.33	64 × 0.6‡	1.1	21.1	63	20	Fast
GE*	0.7	64 × 0.625	0.5625	22.5	32	40	Slow
GE*	0.6	64 × 0.625	0.9375	37.5	63	20	Fast

* Sixty-four–channel GE scanners not been used in practice by the authors at time of writing.
† Scan times shown for a scanning range of 130 cm.
‡ Physical detector configuration is 32 detector rows.
§ Scan time fixed to 40 sec.

peripheral arterial tree can be acquired if 1.25–2-mm-thick sections are reconstructed at 0.8–1-mm intervals (**Fig 4**). However, the acquisition speed with these parameter settings is substantially faster compared with four- and eight-channel systems. In fact, it may be too fast for patients with altered flow dynamics (as detailed later). Therefore, in contrast to four- and eight-channel CT, it is generally not necessary and potentially detrimental to choose the maximum pitch and/or the fastest gantry rotation speed with these scanners.

Sixteen-channel CT also allows, for the first time, acquisition of submillimeter "isotropic" data sets of the entire peripheral arterial tree. With detector configuration settings such as 16 × 0.625 mm or 16 × 0.75 mm, it is possible to reconstruct sections less than 1 mm in thickness spaced every 0.5–0.8 mm. With these settings, the acquisition speed is somewhat slower, in the range of 40–50 seconds, which is comparable to routine four-channel (4 × 2.5 mm) and eight-channel (8 × 1.25 mm) system acquisitions. These isotropic resolution data sets further improve the visualization of small crural or pedal vessels; however, image noise and increased dose and tube current requirements may be problematic in the abdomen unless automated tube current modulation is available.

However, it is important to bear in mind that submilllimeter acquisition (16 × 0.625 mm, 16 × 0.75 mm) does not necessarily require submillimeter image reconstruction (ie, reconstructing the thinnest possible images). For example, one might routinely choose to reconstruct thicker high-resolution (eg, 1.25 mm) data sets from a submillimeter acquisition. This strategy still allows the user to go back and reconstruct another isotropic submillimeter data set at maximum spatial resolution if clinically necessary. It is our experience that the reconstruction of a single high-resolution data set (approximately 1.25–1.5 mm section thickness) obtained with eight- and 16-channel CT and 1-mm section thickness with 64-channel CT provides adequate spatial resolution for the entire peripheral arterial tree while keeping the noise level in the abdomen and pelvis within an acceptable range.

Sixty-four–channel CT

Data acquisition with 64-channel CT normally ensues on a submillimeter scale (64 × 0.6 mm or 64 × 0.625 mm). Because of peripheral arterial enhancement dynamics, it is important to deliberately slow the acquisition speed with these scanners by selecting a low pitch and refraining from using the maximum gantry rotation speed, most notably in patients with stenoocclusive disease.

Again, one can use the raw data from the submillimeter acquisition to routinely reconstruct data sets with a section thickness of 1.0–1.5 mm (ie, high-resolution; **Fig 5**). Submillimeter isotropic images with a section thickness as small as 0.6–1.0 mm, spaced every 0.4–0.7 mm, may be reconstructed from the same acquisition. This maximum spatial resolution may translate into improved visualization and treatment planning of patients with advanced peripheral arterial occlusive disease.

Peripheral CT angiography data sets are generally large, ranging from 900 to 2,500 images. We currently save all images in our Picture Archiving and Communication System, but this may not be feasible for all institutions. One potential solution to reduce file sizes is to permanently archive 1.5–2-mm-thick images, and use thinner sections (eg, submillimeter) for data viewing only and for the generation of

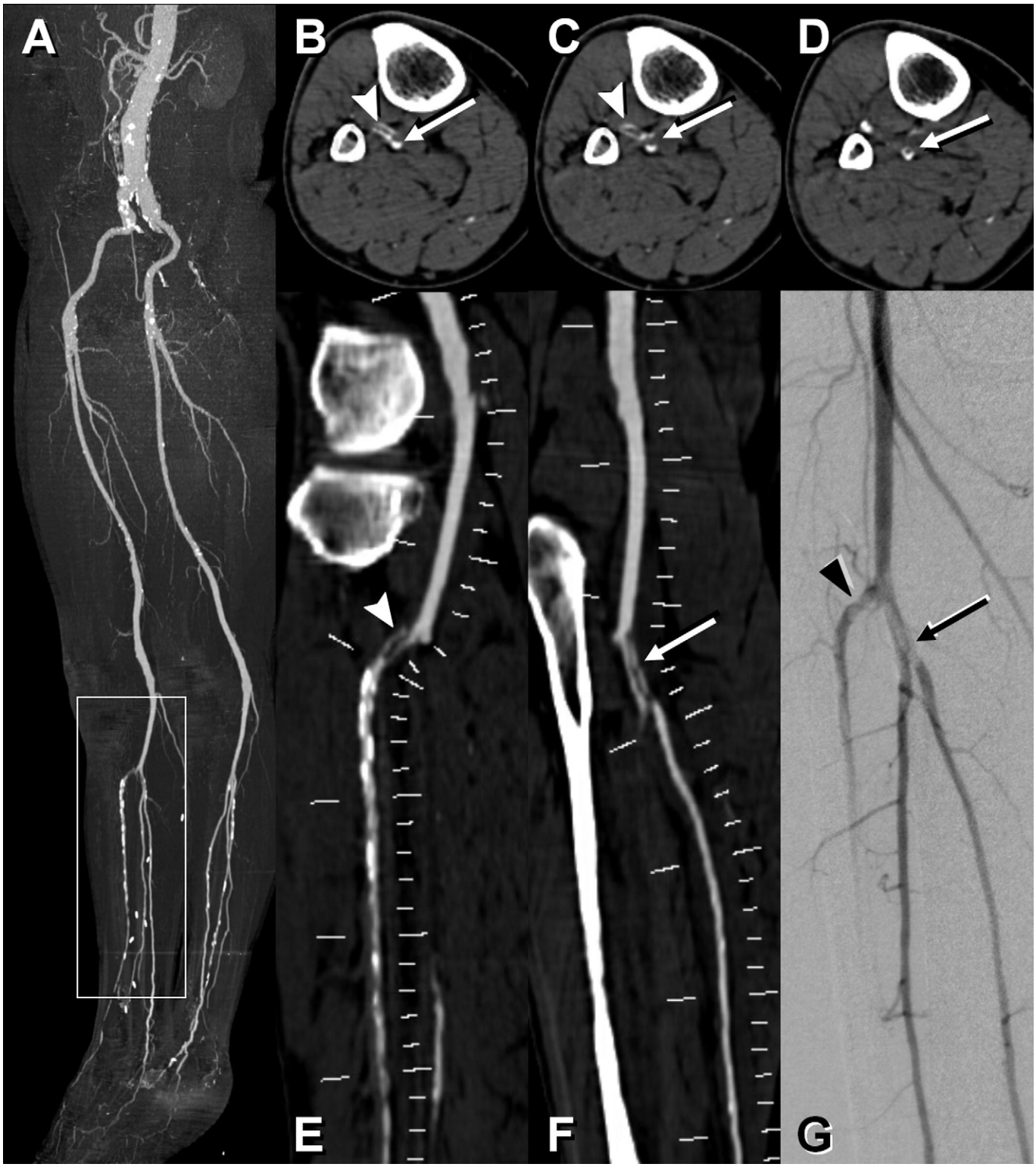

Figure 2. Four-channel CT (4 × 2.5 mm, 3.0 mm/1.0 mm) peripheral CT angiogram of a 62-year-old man with abdominal and bilateral common iliac artery aneurysms and subacute onset of right foot pain. **(a)** Oblique (45° left anterior oblique) MIP image of entire data set. Box indicates magnified views. **(b–d)** axial CT images through the right proximal calf show embolic filling defects in the anterior tibial artery (arrowheads) and the tibioperoneal trunk (arrows). **(e,f)** Corresponding CPR images from the popliteal artery through the anterior tibial artery **(e)** and posterior tibial artery **(f)** display intraluminal filling defects. DSA confirms CT angiography findings **(g)**.

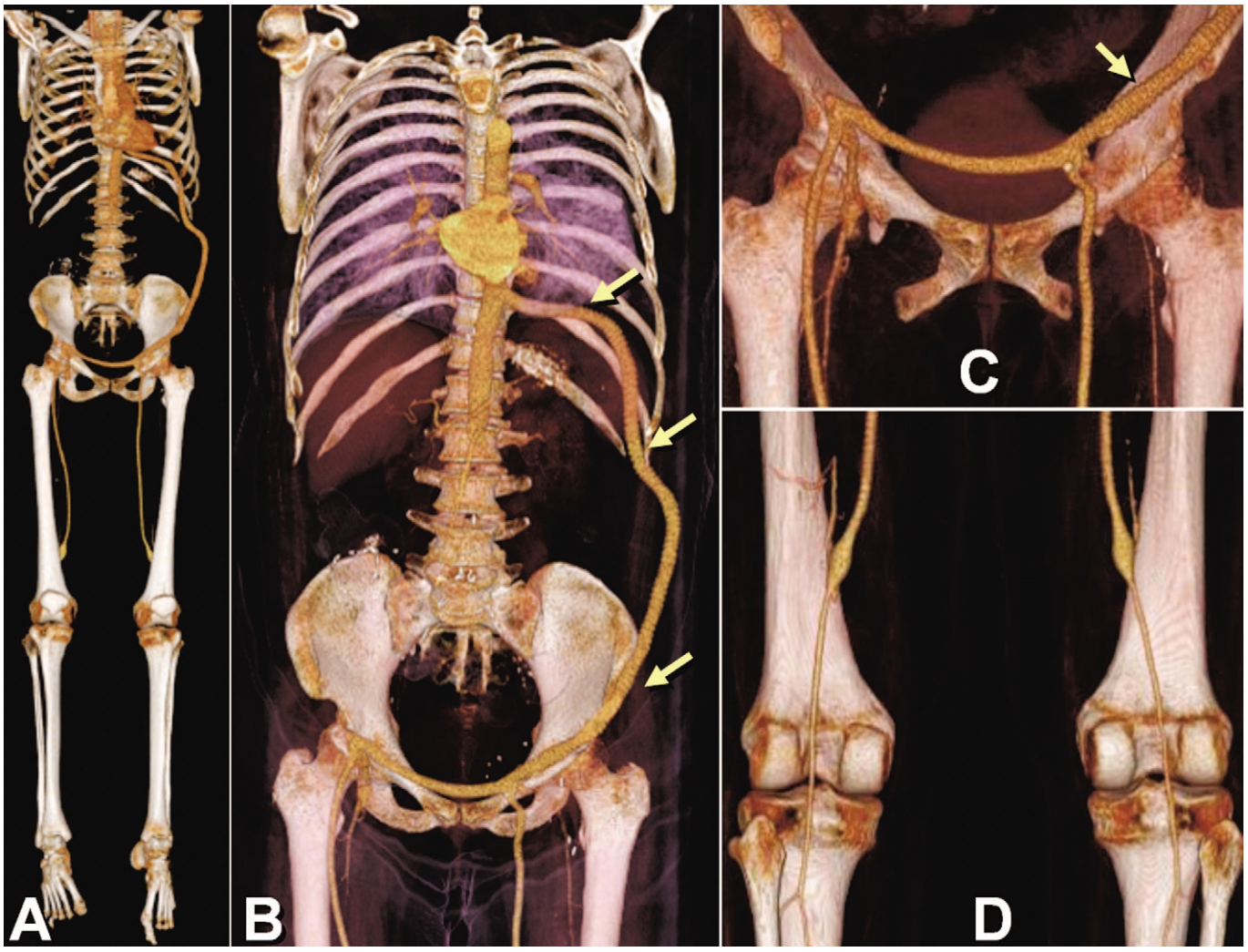

Figure 3. Eight-channel CT angiogram (8 × 1.25 mm, 1.25 mm/0.9 mm) of the chest, abdomen, pelvis, and lower-extremity arteries (length, 150 cm) obtained in 45 seconds with use of a pitch of 1.675 **(a)**. This 48-year-old woman with an occluded right axillofemoral bypass (not opacified) was referred for surveillance of a recent thoracic aortobifemoral bypass (**b**) and bilateral femoropopliteal bypass grafts **(c,d)**.

permanent high-quality reformatted images.

Contrast Medium Injection Technique

Intravenous contrast medium is injected with a power injector into an antecubital vein with use of a 20-gauge intravenous cannula. The basic principles of contrast medium injection for CT angiography, such as the relationship of the injection flow rate and the injection duration on arterial enhancement, also apply to peripheral CT angiography, at least for its aortoiliac portion (14). However, peripheral CT angiography is more complex with respect to synchronizing the enhancement of the entire lower-extremity arterial tree with the CT data acquisition speed.

One to 1.5 g of iodine injected per second usually achieves adequate arterial enhancement for an average (75 kg) person. Body weight–based adjustments of the injection flow rate and volume are recommended, at least for those subjects who weigh more than 90 kg or less than 60 kg. The injection duration also affects the time course of arterial enhancement. With a continuous intravenous injection of contrast medium over a prolonged period of time (eg, 35 seconds), arterial enhancement continuously increases over time (15). This explains why the attenuation values observed in peripheral CT angiograms are usually lowest in the abdominal aorta and peak at the level of the infragenicular popliteal artery (7). In general, biphasic injections result in more uniform enhancement over time, notably with long scan and injection times (>25–30 seconds) (16).

Principles of Scan Timing

The time interval between the beginning of an intravenous contrast material injection and the arrival of the bolus in the aorta, referred to as the contrast medium transit time, is very

Figure 4. Sixteen-channel CT (16 × 1.25 mm, 1.25 mm/0.8 mm) peripheral CT angiogram in a 70-year-old man with right thigh claudication and right iliofemoral artery occlusion demonstrates exquisite detail of small collateral vessels **(a)**, as well as femoropopliteal **(b)**, pedal **(c)**, and crural arteries **(d)**.

variable among patients with coexisting cardiocirculatory disease, and may range from 12 to 40 seconds. Individualizing the scanning delay is therefore generally recommended in peripheral CT angiography. A patient's individual contrast medium transit time can be reliably determined with a small test bolus injection or estimated with use of automated bolus triggering techniques. The scanning delay may then be chosen to equal the contrast medium transit time (the scan is therefore initiated as soon as contrast medium arrives in the aorta), or the scanning delay may be chosen at a predefined interval after the contrast medium transit time. For example, the notation "contrast medium transit time + 5 seconds" means that the scan starts 5 seconds after contrast medium has arrived in the aorta.

Aortopopliteal Bolus Transit Times

The additional challenge in patients with peripheral arterial occlusive disease is related to the well-known fact that arterial stenoses, occlusions, or aneurysms anywhere between the infrarenal abdominal aorta and the pedal arteries may substantially delay downstream vascular opacification (17,18). More specifically, we found in a group of 20 patients with peripheral arterial occlusive disease that the transit times of intravenously injected contrast medium to travel from the aorta to the popliteal arteries to range from 4 seconds to 24 seconds (mean, 10 sec), which corresponds to bolus transit speeds as fast as 177 mm/sec to as slow as 29 mm/sec, respectively (19).

The clinical implication for peripheral CT angiography is that when a table speed of approximately 30 mm/sec is selected, it is very unlikely (although not impossible) that the data acquisition is faster than the intravascular contrast medium bolus. However, with increasing acquisition speeds, the scanner table may move faster than the intravascular contrast medium column, and the scanner may therefore "outrun" the bolus. Of note, outrunning the bolus has been reported in only one study to our knowledge, which used a table speed of 37 mm/sec (9), but it has not been reported in five other published studies on peripheral CT angiography, all of

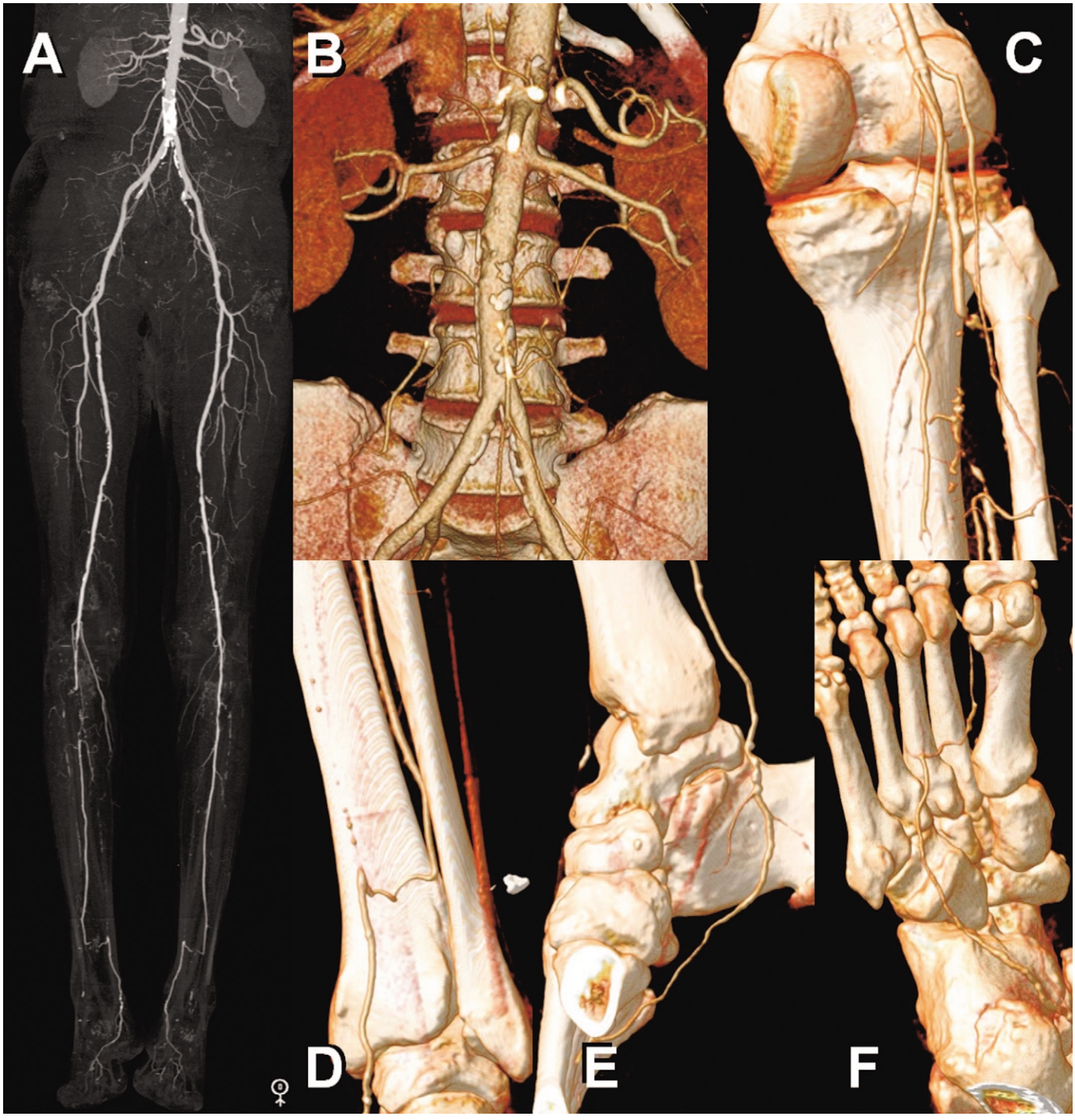

Figure 5. Sixty-four–channel CT (64 × 0.6 mm, 1.0 mm/0.7 mm) peripheral CT angiogram in an 83-year-old man with right side–dominant calf and foot claudication. Automated tube current modulation (CareDose 4D; Siemens) allows submillimeter acquisition and reconstruction with acceptable image noise level in the abdomen and unprecedented spatial resolution down to the plantar arch and metatarsal branches. MIP of the entire data set **(a)**; VR views of the abdomen **(b)** and right leg runoff **(c–f)** show distal aortic calcific plaque and patent renal arteries **(b)** occlusion of the right popliteal trifurcation with reconstitution of the peroneal artery **(c)**, which reconstitutes the right posterior tibial artery above the ankle via a communicating branch **(d)**, and supplies the foot through the common and lateral plantar arteries **(e)** which fill the plantar arch **(f)**.

Table 2
Peripheral CTA Injection Protocol for Slow Acquisitions

Parameter	Specification
Table speed	≤ 30 mm/sec
Scanning time	≥ 40 seconds
Examples of acquisition parameters	4 × 2.5 mm, 8 × 1.25 mm, 16 × 0.75 mm, 16 × 0.625 mm, 64 × 0.6 mm, 64 × 0.625 mm (slow pitch and gantry rotation; see Table 1)
Injection duration	Scan time minus 5 seconds (≥35 sec)
Scanning delay	Equal to contrast medium transit time (contrast material arrival in the aorta, as determined by a test bolus or automated bolus triggering)
Injection flow rates	
Biphasic	5–6 mL/sec (1.8 gI/sec) for 5 seconds, plus 3–4 mL/sec (1.0 gI/sec) for remaining seconds (scan time minus 10)
Example: for an acquisition time of 45 seconds, inject	30 mL at 6 mL/sec plus 115 mL at 3.3 mL/sec (300 mgI/mL concentration contrast medium); 25 mL at 4.5 mL/sec plus 85 mL at 2.5 mL/sec (400 mgI/mL concentration contrast medium); Total injection duration is 35 sec (5 sec plus 30 sec) Total CM volume is 145 mL or 110 mL, respectively

Note.—Injection flow rates vary depending on the iodine concentration of the contrast agent used. Iodine injection rate is adequate for a 75-kg individual and should be increased or decreased for subjects who weigh more than 90 kg or less than 60 kg.

which used table speeds of 19–30 mm/sec (7,8,10,11,20).

For the following discussion, it is therefore useful to arbitrarily categorize injection strategies for peripheral CT angiography into those for slow acquisitions (≤30 mm/sec table speed), and those for fast acquisitions (>30 mm/sec table speed). Sixty-four–channel CT injection strategies will be discussed separately.

Table 3
Peripheral CT Angiographic Injection Protocol for Fast Acquisitions in Patients with Peripheral Arterial Occlusive Disease

Parameter	Specification
Table speed	> 30 mm/sec
Scanning time	< 40 sec
Examples of acquisition parameters	8 × 2.5 mm 16 × 1.25 mm, 16 × 1.5 mm, 64 × 0.6 mm, 64 × 0.625 mm (for pitch and rotation; see Table 1)
Injection duration	35 sec
Scanning delay:	Contrast medium transit time plus (40 sec minus scanning time)*
Injection flow rates:	1.5 gI /sec (4–5 mL/sec)
Examples:	Always inject for 35 seconds, eg 140 mL at 4 mL/sec For a scan time of 30 sec, start scanning 10 sec after contrast medium arrived in aorta; For a scan time of 25 sec, start scanning 15 sec after contrast medium arrived in aorta; For a scan time of 20 sec, start scanning 20 sec after contrast medium arrived in aorta

Note.—The term "40 sec minus scanning time" is also referred to as the diagnostic delay. Iodine injection rate of 1.5 g/sec is adequate for a 75-kg individual, and should be increased/decreased for subjects who weigh more than 90 kg or less than 60 kg (20 mgI/kg body weight/sec). Injection flow rates will vary depending on iodine concentration of contrast medium.

Injection Strategies for Slow Acquisitions

Detector configuration settings of 4 × 2.5 mm, 8 × 1.25 mm, and 16 × 0.625 mm all translate into acquisition speeds of approximately 30 mm/sec. Such a table speed usually translates into a scan time of approximately 40 seconds for the entire peripheral arterial tree. Because the data acquisition follows the bolus from the aorta down to the feet, the injection duration can be chosen to be approximately 5 seconds shorter than the scan time. For example, for a 40-second acquisition, a 35-second injection duration is sufficient. This would translate into 140 mL of contrast medium if a constant injection rate of 4 mL/sec was used. If the beginning of the data acquisition is timed closely to the contrast medium arrival time in the aorta (with use of a test bolus or bolus triggering), biphasic injections achieve more favorable enhancement profiles with improved aortic enhancement. As an example, our current protocol for a submillimeter acquisition with a Siemens 16-channel scanner is shown in (**Table 2**). A similar concept is used for the 64-channel Siemens scanner at our institution as well (as described later).

Because the possibility of even more delayed arterial opacification than accounted for in the aforementioned protocol cannot be excluded (19), a second CT angiography acquisition (covering the popliteal and infrapopliteal vasculature) should be preprogrammed into the scanning protocol (**Fig 1**). This acquisition is initiated by the CT technologist immediately after the main CT angiography acquisition only if he or she does not see any contrast medium opacification in the distal vessels.

Injection Strategies for Fast Acquisitions

Detector configuration settings of 8 × 2.5 mm, 16 × 1.25 mm, or 16 × 1.5 mm translate into acquisition speeds of 45–65 mm/sec, which, in some individuals, may be faster than the contrast medium bolus travels through a diseased peripheral arterial tree. To

Table 4
Weight-based Biphasic Injection Protocol for 64-Channel Peripheral CT Angiography for Patients with Peripheral Arterial Occlusive Disease

Parameter	Specification
Table speed	Variable (approximately 30 mm/sec) depending on longitudinal coverage
Scanning time	40 sec (all patients)
Acquisition parameters	64 × 0.6 mm Gantry rotation period: 0.5 sec; pitch usually ≤ 1 120 kV, 250 quality reference mA (CareDose 4D)
Injection duration	35 sec (all patients)
Scanning delay	Contrast medium transit time + 3 sec (minimum delay with CareBolus, including breath-hold command)
Biphasic injection	Maximum flow rate for first 5 seconds of injection, continued with 80% of this flow rate for 30 seconds and a saline solution flush
<55 kg body weight	20 mL (4.0 mL/sec) + 96 mL (3.2 mL/sec)
<65 kg body weight	23 mL (4.5 mL/sec) + 108 mL (3.6 mL/sec)
75 kg body weight*	25 mL (5.0 mL/sec) + 120 mL (4.0 mL/sec)
>85 kg body weight	28 mL (5.5 mL/sec) + 132 mL (4.4 mL/sec)
>95 kg body weight	30 mL (6.0 mL/sec) + 144 mL (4.8 mL/sec)

* Average.

prevent the CT acquisition to outrun the bolus, it is necessary to allow the bolus a "head start." This is accomplished by combining a fixed injection duration of 35 seconds to fill the arterial tree with a delay of the start of the CT acquisition relative to the time of contrast medium arrival in the aorta. The faster the acquisition, the longer this diagnostic delay should be. We use such a strategy with a GE 16-channel scanner with a 16 × 1.25 mm protocol, pitch of 1.375, and 0.6 seconds gantry rotation period (table speed, 45 mm/sec). The protocol, as well as its generalization to other fast acquisitions, is shown in **Table 3**. Examples of arterial opacification with use of this approach on fast scans are shown in **Figure 4**. The limitation of the use of a very long diagnostic delay (>15 seconds between contrast medium arrival and scan initiation) is undesirable opacification of the renal and portal veins and the inferior vena cava.

Injection Strategy for 64-Channel CT

Whereas 32-, 40-, and 64-channel CT systems theoretically allow acquisition speeds of 80 mm/sec and more, we deliberately acquire our peripheral CT angiograms at a much slower pace by prescribing a fixed scan time of 40 seconds for each individual. For a 40-second scan time, we select a gantry rotation of 0.5 seconds and a pitch of less than 1. Automated tube current modulation is used in this setting to avoid increased radiation dose. The advantage of always selecting the same 40-second scan time is that it can be combined with fixed (biphasic) injections for 35 seconds. The injection flow rates and volumes are then individualized to patient weight (**Table 4**). Examples of image quality and opacification are shown in **Figure 5**.

All these acquisition and contrast medium injection strategies reduce the risk of outrunning the bolus; however, this is not entirely excluded. **Figure 6** shows an example of a patient with extremely delayed flow, most likely caused by decreased cardiac output and altered flow dynamics resulting from bilateral iliac and popliteal artery aneurysms and diffuse arteriomegaly.

Other Injection Strategies

The aforementioned injection strategies combine individual scan timing (with use of bolus tracking/test bolus) in the aorta, with empiric (ie, nonindividualized) parameter selection to adjust for a broad range of possible bolus transit speeds down to the feet. Other approaches with use of more or less individualization are also possible. For example, protocols with a fixed, long scanning delay (eg, 28 seconds) have been used successfully in the past, notably before automated bolus tracking technique was available on the first four-channel scanners (11). On the other end of the spectrum are attempts to individualize the scanning delay and the scanning speed based on aortic and popliteal transit times, determined individually with two test boluses (21).

Venous Enhancement

Opacification of deep and superficial veins can be observed in peripheral CT angiography (7) and is more likely to occur with longer scan times and in patients with active inflammation, such as that from infected or nonhealing ulcers. Given the rapid arteriovenous transit times observed angiographically in some patients (22), venous opacification cannot be completely avoided. Because arterial enhancement is always stronger than venous enhancement when the injection is timed correctly (7), and with adequate anatomic knowledge and postprocessing tools, venous enhancement rarely poses a diagnostic problem.

Visualization and Image Interpretation

Visualization, image interpretation, and effective communication of findings are demanding in peripheral CT angiography. A powerful medical image postprocessing workstation, as well as standardized workflow and visualization protocols, are required when peripheral CT angiograms are obtained on a regular basis.

Various two- and three-dimensional (3D) postprocessing techniques are available on today's state-of-the-art workstations. For patients with atherosclerotic disease, a combination of 3D overview techniques with at least one two-dimensional cross-sectional technique is generally required. The selection of postprocessing techniques not only depends on the type of disease, but also on the specific visualization goal: interpretation versus documentation. In the context of interactive exploration of the data sets, usually done by the radiologist interpreting the study during readout, fast navigation and flexible visualization tools are preferred. In the setting of

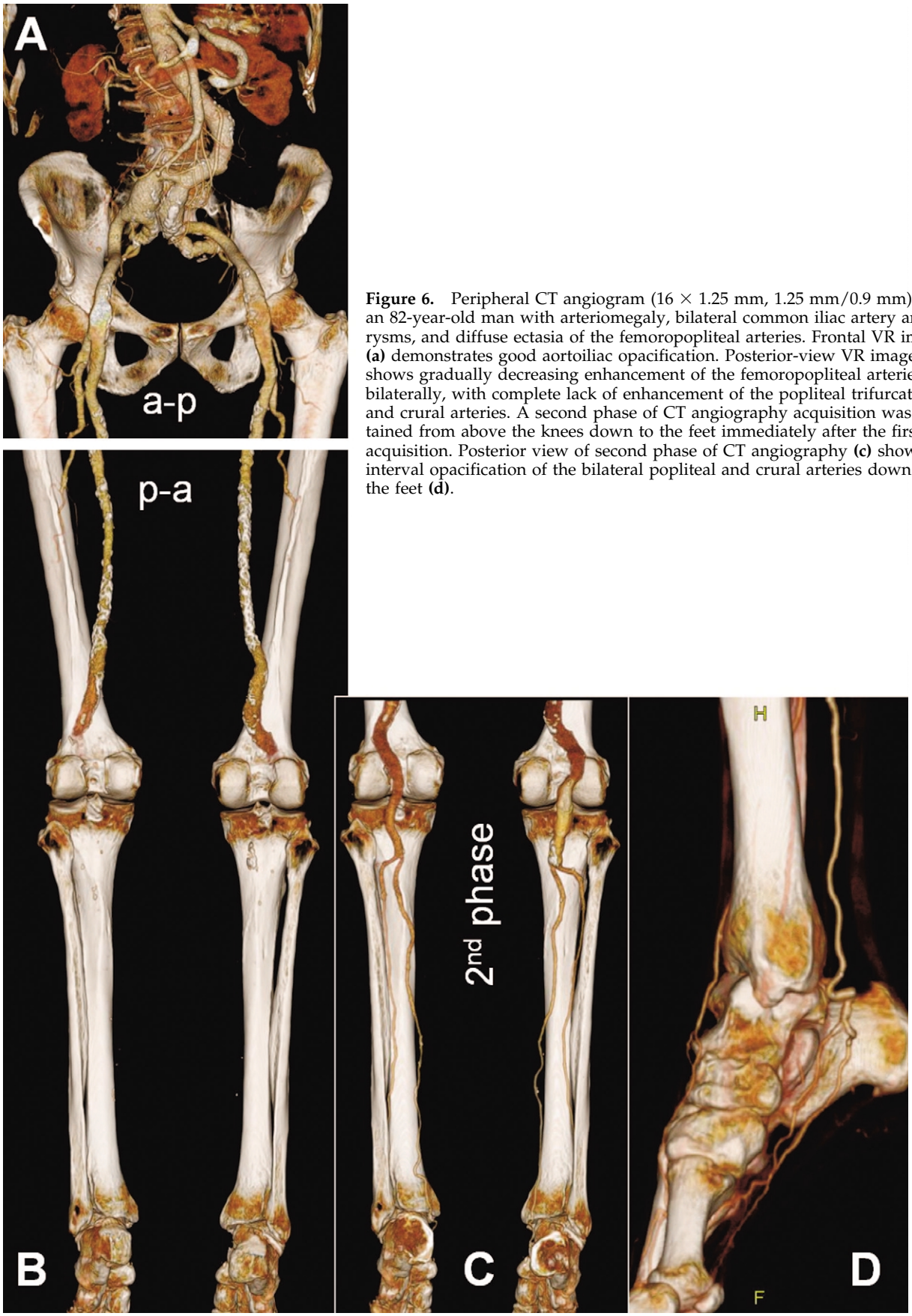

Figure 6. Peripheral CT angiogram (16 × 1.25 mm, 1.25 mm/0.9 mm) in an 82-year-old man with arteriomegaly, bilateral common iliac artery aneurysms, and diffuse ectasia of the femoropopliteal arteries. Frontal VR image **(a)** demonstrates good aortoiliac opacification. Posterior-view VR image **(b)** shows gradually decreasing enhancement of the femoropopliteal arteries bilaterally, with complete lack of enhancement of the popliteal trifurcation and crural arteries. A second phase of CT angiography acquisition was obtained from above the knees down to the feet immediately after the first acquisition. Posterior view of second phase of CT angiography **(c)** shows interval opacification of the bilateral popliteal and crural arteries down to the feet **(d)**.

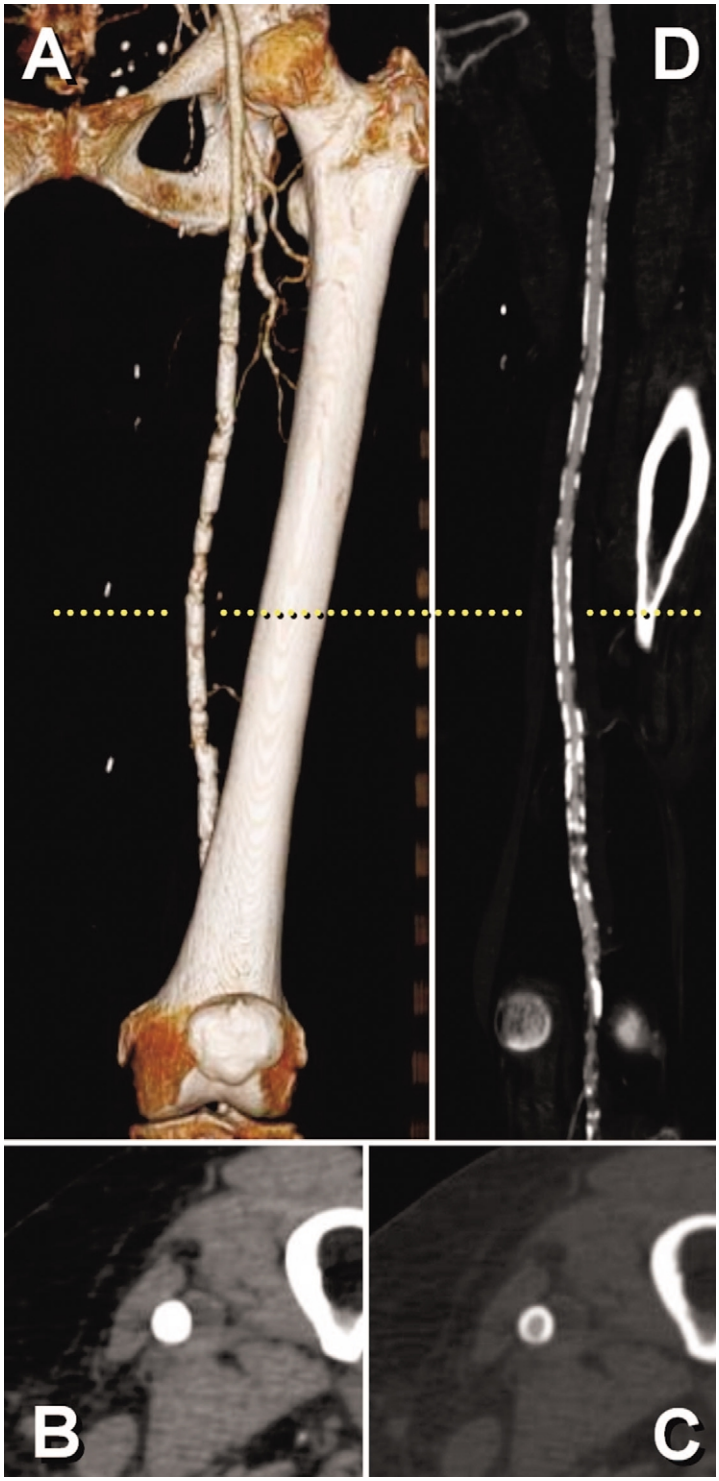

Figure 7. Peripheral CT angiography (16 × 1.25 mm, 1.25 mm/0.9 mm) in a 72-year-old woman with nonhealing left forefoot ulcer. **(a)** VR image of the left superficial femoral artery shows excessive vessel wall calcifications, precluding the assessment of the flow channel. Cross-sectional views were required to visualize the vessel lumen. Axial CT images **(b,c)** through the mid-superficial femoral artery (dotted line in **a** and **d**) with viewing window settings (level/width) of 200 HU/600 HU **(b)** does not allow us to distinguish between opacified vessel lumen and vessel calcification, which can be distinguished only when an adequately wide window width (300 HU/1,200 HU) is used **(c)**. Similar wide window settings are also used for a CPR through the same vessel **(d)**, displaying several areas of wall calcification with and without stenosis.

creating standardized sets of static images and measurements for documentation and communication, techniques that allow a protocol-driven generation of predefined views are preferred. The typical protocol for postprocessing of peripheral CT angiography in our 3D laboratory consists of curved planar reformations (CPRs); thin-slab maximum-intensity projections (MIPs) through the renal and visceral arteries; bone removal; full-volume MIPs and volume renderings (VRs) of the abdomen, pelvis, and each leg; and filming and archiving of these views. Although the creation of such sets of images may be time-consuming even for an experienced technologist, the clinical interpretation is fast and straightforward for the image recipient.

Transverse Source Image Viewing

Reviewing of transverse CT slices is mandatory for the assessment of extravascular abdominal or pelvic pathologic processes. This is facilitated by reconstructing an additional series of contiguous 5-mm-thick sections through the abdomen and pelvis. Browsing through the stack of source images is also helpful to gain a first impression of vascular abnormalities, and in select cases, such as in patients with minimal or absent disease or patients with trauma or suspected acute occlusions, source image viewing may be sufficient to completely address the concern (**Fig 2**). Axial images also display relevant extravascular anatomy, such as the course and position of the medial head of the gastrocnemius muscle in popliteal entrapment syndrome, which may not be apparent on images such as MIPs. Source images may also serve as a reference when two-dimensional or 3D reformatted images suggest artifactual lesions. However, for the majority of cases with vascular disease, transverse image viewing is inefficient and less accurate than viewing reformatted images (10).

Postprocessing Techniques

MIP.—Assessment of vascular abnormalities is facilitated when the arterial tree is displayed in an angiographic fashion. This can be accomplished with MIP or VR techniques. MIP provides the most "angiogra-

phy-like" display of the vasculature, particularly when no or minimal vessel calcifications are present. MIP is therefore ideal for communicating findings to the referring services and for creation of a "road map" for treatment planning within the angiography suite or the operating room (**Figs 2,5**). The disadvantage of MIP is that it requires that bones are removed from the data set, and even with the help of automated or semiautomated computer algorithms on modern workstations, this remains a time-consuming task. Additionally, inadvertent removal of vessels in close vicinity to bony structures may lead to spurious lesions.

Volume rendering.—Because VR preserves 3D depth information, unlike MIP, bone editing may not be required. Rather than editing the bones out of the data set, one can use clip planes or volume slabs together with interactive selection of the appropriate viewing angles to expose the relevant vascular segment. Interactive adjustment of the opacity transfer function allows the user to blend in or carve out exquisite vascular detail when necessary. VR is the ideal tool for fast interactive exploration of peripheral CT angiography data sets. Although "snapshot" views obtained during data exploration can be invaluable for communicating a specific finding or detail, VR is somewhat less suited for standardized documentation of images. In part, this is because most Picture Archiving and Communication System workstations do not display the color information on high-resolution grayscale monitors.

The main limitation of MIP and VR is that vessel calcifications and stents may completely obscure the vascular flow channel (**Fig 7**). This fundamental limitation precludes the exclusive use of these techniques in a substantial proportion (approximately 60%) of patients with peripheral arterial occlusive disease (23).

Multiplanar reformation and CPR.—In the presence of calcified plaque, diffuse vessel wall calcification, or endoluminal stents, cross-sectional views are essential to assess the vascular flow channel (**Fig 7**). Transverse source images, sagittal, coronal, or oblique multiplanar reformations (MPRs) are useful in an interactive setting, such as in conjunction with VR.

Alternatively, longitudinal cross-sections along a predefined vascular center line, ie, CPR, can be created (**Fig 8**). CPRs provide the most comprehensive cross-sectional display of luminal pathologic processes, but require manual or (semi-)automated tracing of the vessel center lines (24,25). CPR does not require bone editing, but at least two CPRs per vessel segment (eg, sagittal and coronal views) have to be created to fully evaluate eccentric disease.

One problem of (single) CPR images in the context of visualizing the peripheral arterial tree is their limited spatial perception. With bony landmarks out of the curved reconstruction plane, the anatomic context of a vascular lesion may be ambiguous unless clear annotations are present. This limitation has recently been alleviated by an extension of standard CPR to so-called multipath CPR images (24). Multipath CPR images provide simultaneous longitudinal cross-sectional views through the major conducting vessels (**Fig 9**) without obscuring vessel wall calcifications and stents, while maintaining spatial perception (26). We are currently evaluating this technique as a routine clinical visualization, documentation, and endovascular treatment-planning tool for peripheral CT angiography.

Thin-slab MIP, thin-slab VR, and thick MPR/CPR.—If applied to subvolumes of the data sets with use of clip planes or slabs of the volume to focus on a particular area of interest, the resulting images are referred to as thin-slab MIPs, thin-slab VRs, or thick MPRs (or CPRs) (27,28). Interactive real-time variation of the viewing direction, the thickness of the rendered volume, adjustments to window-level settings or opacity transfer functions, etc, is ideal for interactively exploring the data sets.

Automated Techniques for Segmentation and Visualization

Although fully automated detection of vessel centerlines, automated segmentation of bony structures, and detection (and subtraction) of vessel wall calcification are highly desirable, no such algorithms have yet been developed. This is not surprising when considering the complex manifestations of vascular disease; the wide range of vessel sizes; the wide overlap in CT density values of opacified blood, plaque, and low-attenuation bone; and the inherently limited spatial resolution and image noise in peripheral CT angiography data sets. Although traditional density- and gradient-based algorithms are unlikely to completely solve the problem in the near future, several software tools for improved and faster editing and for creating center lines through the arteries have been developed and are available on modern 3D workstations.

At this point it is therefore reasonable to expect further improvements in computer-assisted segmentation and visualization in the near future, but it would be naïve to expect that expert user interaction, such as by a radiologist or 3D imaging technologist, can be completely avoided in the creation of clinically relevant and representative images.

Interpretation and Pitfalls

Vascular abnormalities have to be interpreted in the context of a patient's symptoms and stage of disease, and with respect to the available treatment options. For those familiar with reading conventional angiograms, the clinical aspect of interpreting a peripheral CT angiogram is usually straightforward. However, visual perception and interpretation of well-known abnormalities in a new and different format (such as VR or CPR images) requires adaptation and familiarity with the specific techniques used.

Probably the most important pitfall related to the interpretation of peripheral CT angiograms is related to the use of narrow viewing window settings in the presence of arterial wall calcifications or stents. Even at wider-than-normal CT angiographic window settings (window level/width, 150/600 HU), high-attenuation objects (eg, calcified plaque, stents) appear larger than they really are ("blooming" caused by the point-spread function of the scanner), which may lead to an overestimation of a vascular stenosis or suggest a spurious occlusion. When scrutinizing a calcified lesion or a stent-implanted segment with use of any of the cross-sectional grayscale

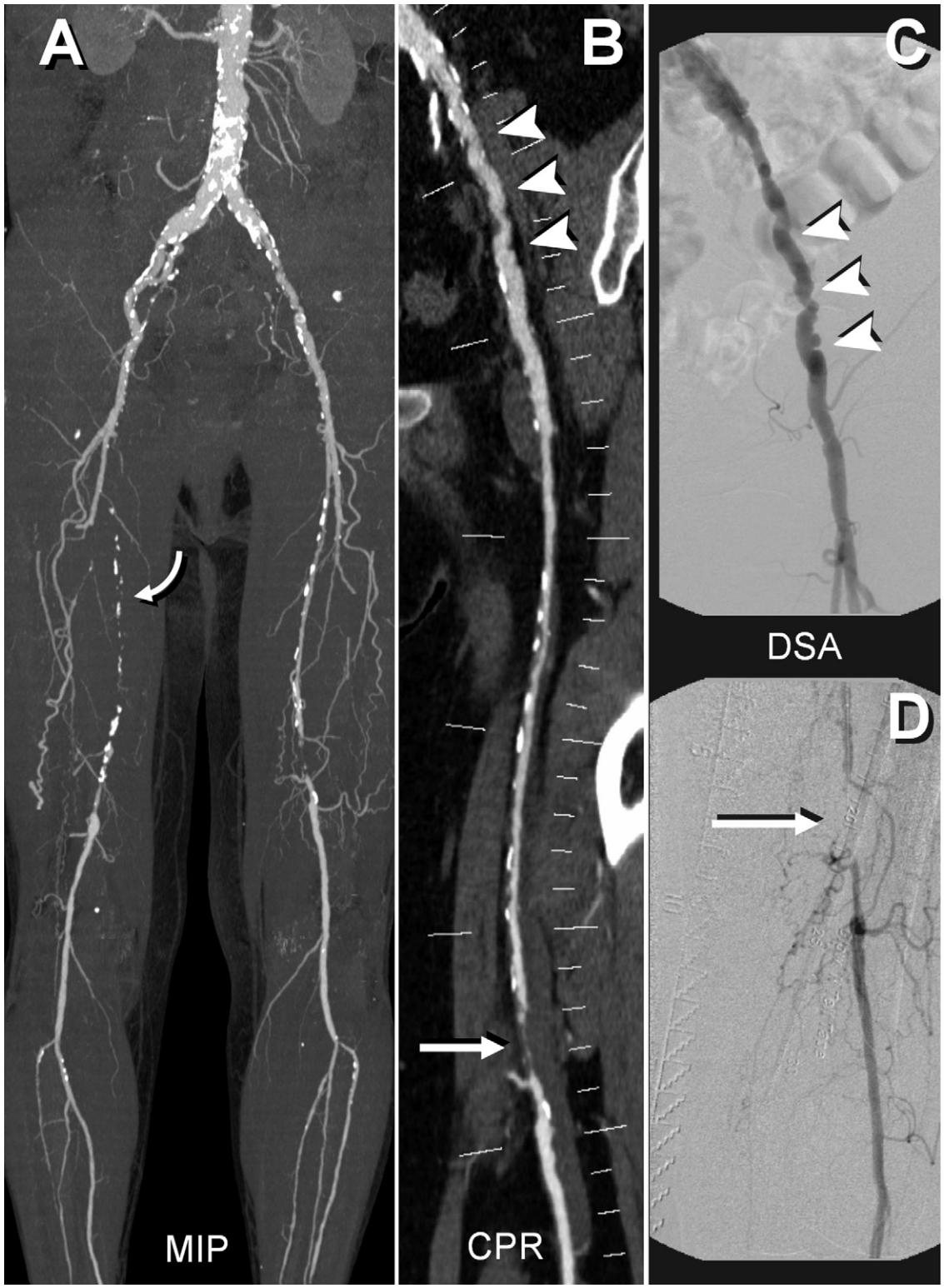

Figure 8. Peripheral CT angiography (16 × 0.75 mm, 2.0 mm/1.0 mm) in a 73-year-old woman with intermittent claudication bilaterally. MIP **(a)** shows long right femoropopliteal occlusion (curved arrow) and diffuse disease of the left superficial femoral artery with a short distal near-occlusion. CPR **(b)** through left iliofemoral arteries demonstrates multiple mild stenoses of the external iliac artery (arrowheads), a diffusely diseased left superficial femoral artery, and short (<3 cm) distal left superficial femoral artery occlusion. Corresponding selective DSA images of the left external iliac artery **(c)** and the distal left superficial femoral artery **(d)** were obtained immediately before angioplasty/stent implantation.

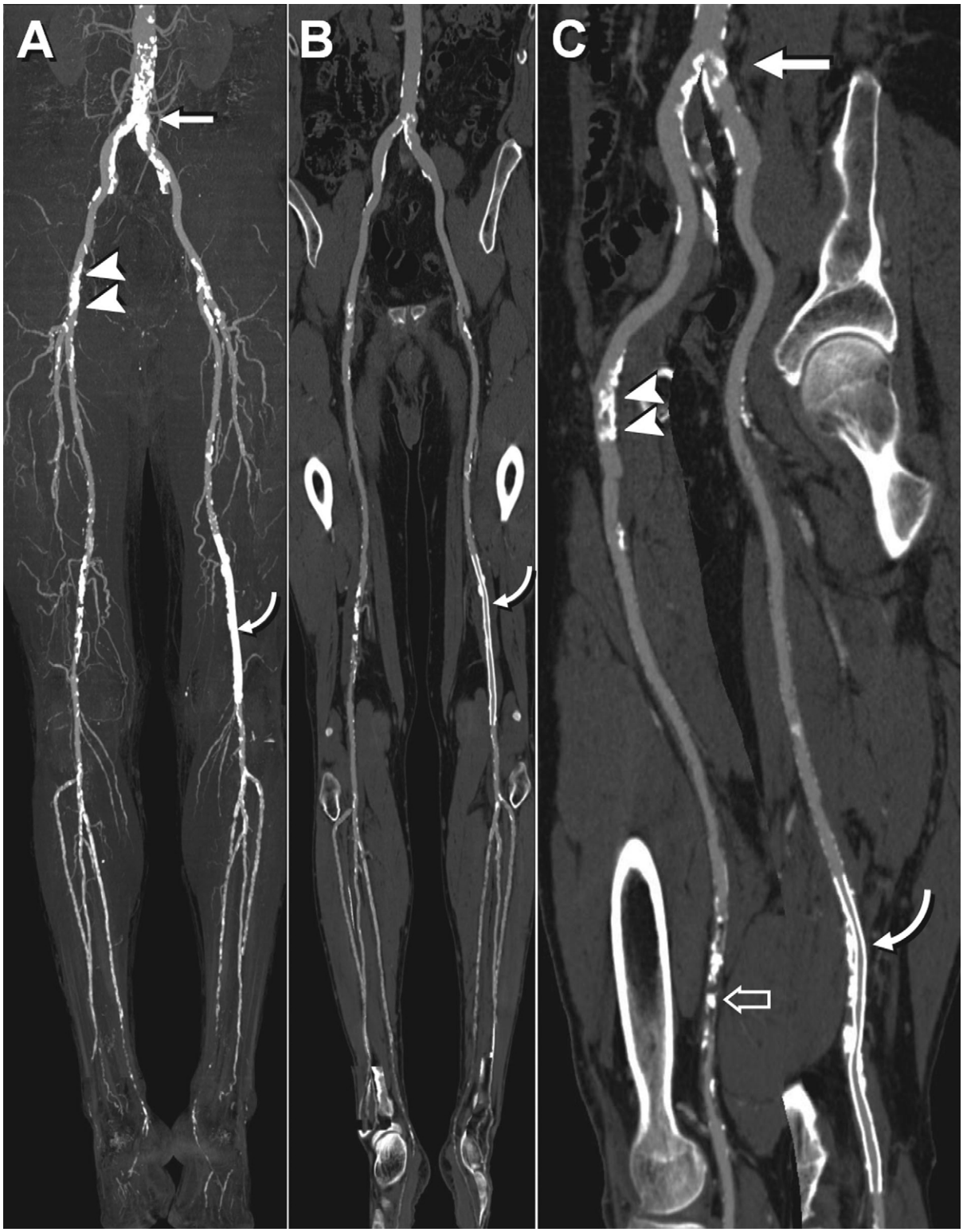

Figure 9. Peripheral CT angiography (16 × 0.75 mm, 2.0 mm/1.0 mm) of a diabetic male patient with bilateral claudication. MIP **(a)** shows arterial calcifications near the aortic bifurcation (arrow), as well as in the right (arrowheads) and left common femoral arteries, in the right femoropopliteal region, and in the crural vessels. A long stent is seen in the left femoropopliteal segment (curved arrow). Frontal view **(b)** and magnified 45° left anterior oblique **(c)** multipath CPR images provide simultaneous CPRs through the aorta and bilateral iliac through crural arteries. Note that prominent calcifications cause luminal narrowing in the proximal left common iliac artery (arrow) and in the right common femoral artery (arrowheads). The left common femoral artery is normal; the long femoropopliteal stent is patent (curved arrow). Mixed calcified and noncalcified occlusion of the right distal femoral artery is also seen (open arrow).

Table 5
Lower-extremity CT Angiography in Comparison with DSA in Patients with Peripheral Arterial Occlusive Disease (8–11,19,20,30)

Study, Year	Collimation (channels × mm)	STh /RI (mm/mm)	No. of Pts.	Sensitivity (%)	Specificity (%)	Accuracy (%)
Ofer et al., 2003 (8)						
>50% stenosis	4 × 2.5	3.2/1.6	18	91	92	92
Occlusion				–	–	–
Martin et al, 2003 (9)						
>75% stenosis	4 × 5	5/2.5	41	92	97	–
Occlusion				89	98	–
Ota et al, 2004 (10)						
>50% stenosis	4 × 2	2/1	24	99	99	99
Iliac/femoral/crural				97/100/100	100/96/100	99/97/100
Occlusion				96	98	98
Catalano et al, 2004 (11)						
>50% steno-occlusion	4 × 2.5	3/3	50	96	93	94
Aortoiliac/femoral/popliteocrural				95/98/96	90/96/93	92/97/94
Portugaller et al., 2004 (20)						
>50% steno-occlusion	4 × 2.5	2.5/1.5	50	92	83	86
Aortoiliac/femoropopliteal/crural				92/98/90	95/70/74	94/88/81
Edwards et al., 2005 (29)						
>50% stenosis	4 × 2.5	3.2/2.0	44	79/72	93/93	–
Occlusion				75/71	82/81	–
Willmann et al., 2005 (30)						
>50% steno-occlusion	16 × 0.75	0.75/0.4	39	96/97	96/97	96/97
Aortoiliac				95/99	98/98	97/98
Femoral				98/97	94/96	96/96
Popliteocrural				96/97	95/96	96/96

Note.—STh/RI = section thickness/reconstruction interval.

images (eg, transverse source images, MPR, or CPR), a viewing window width of at least 1,500 HU may be required (**Fig 7**). Interactive window adjustment on a Picture Archiving and Communication System viewing station or on a 3D workstation are most effective because, when printed on film, window settings are usually too narrow. In the setting of extensive atherosclerotic or media calcification within small crural or pedal arteries, such as those found in diabetic patients and in patients with end-stage renal disease, the lumen may not be resolved regardless of the window/level selection. In these circumstances, other imaging techniques, notably magnetic resonance (MR) imaging, may be preferable to CT angiography.

Other interpretation pitfalls result from misinterpretation of editing artifacts (eg, inadvertent vessel removal) in MIP images and pseudostenosis and/or occlusions in CPRs resulting from inaccurate center-line definition. Most of these artifacts are obvious or easily identified when additional views, complimentary viewing modalities, or source images are reviewed.

Accuracy and Clinical Perspective

For clinical conditions involving the lower-extremity vascular structures, a variety of imaging choices are available. Ultrasound (US), CT angiography, and MR angiography all can provide useful information about lower-extremity arteries and veins noninvasively. The particular modality of choice depends on many factors, including patient demographics and comorbidities, availability and modernity of respective imaging equipment, level of training and confidence of the operating technologists, and local interest and expertise of the radiologist. Each of these factors must be considered when choosing the best imaging examination for an individual patient. Multiple–detector row CT angiography has the advantages of widespread (and increasing) availability, high spatial resolution, and relative freedom from operator dependence.

Lower-extremity CT angiography (introduced in 1998–1999) is the newest technique for peripheral arterial imaging. Therefore, it is not surprising that only sparse original data on its accuracy in patients with peripheral arterial occlusive disease are available (**Table 5**) when compared with the body of published data on US or MR angiography. The majority of published articles on peripheral CT angiography report results with four-channel CT scanners (7–11,29). These small early series do not allow for clinically meaningful stratification of patients into those with claudication and those with limb-threatening ischemia. Other difficulties in interpreting the results of the published literature are the inconsistent thresholds used for grading of significant stenoses, variable categorization of anatomic vessel segments, and use of different visualization and postprocessing tools. All but one group of authors (29) report good overall sensitivities and specificities for the detection of hemodynamically relevant steno-occlusive lesions with four-channel CT relative to intraarterial digital subtraction angiog-

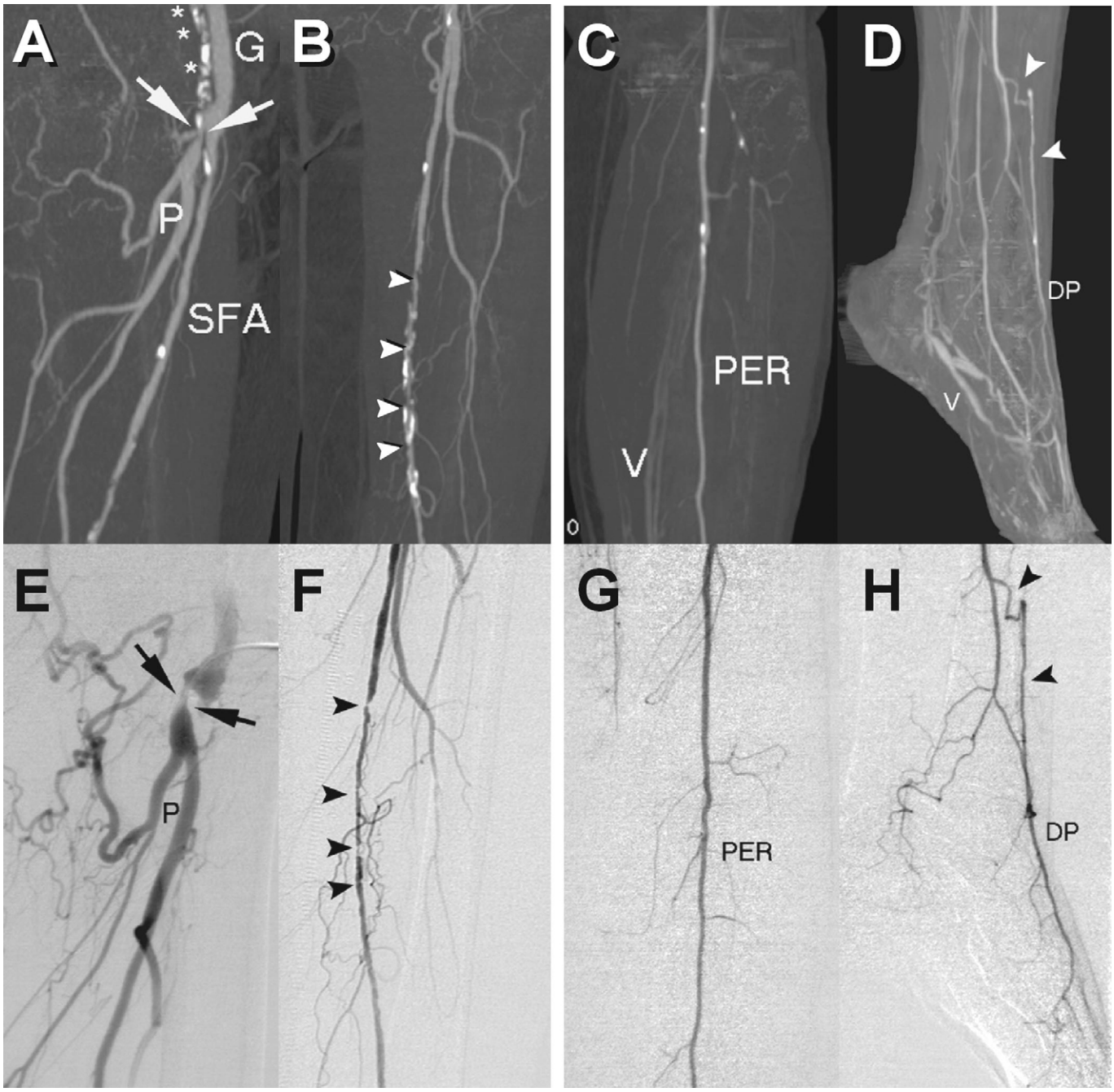

Figure 10. Intermittent left leg claudication in a 62-year-old woman with a history of tobacco use and aortobifemoral bypass grafting. The ankle-brachial index was 0.65. **(a–d)** MIP images with bone segmentation; **(e–h)** DSA images obtained before treatment. **(a)** Oblique MIP image shows high-grade stenosis (arrows) at the origin of the left profunda femoris artery (*P*); a previously placed aortobifemoral graft (*G*) is noted, as is a patent superficial femoral artery (*SFA*). **(b)** Coronal MIP of the left thigh demonstrates multifocal moderate to severe stenosis in the SFA (arrowheads). The SFA is small in caliber with soft and calcified plaque present. **(c)** Coronal MIP of the calf shows a one-vessel runoff (peroneal; *PER*) to the left foot. Mild venous contamination (*V*) is present. **(d)** Sagittal MIP image of the left foot shows collateral vessel reconstitution (arrowheads) of the dorsalis pedis (*DP*) above the ankle from the peroneal artery. **(e)** DSA image from selective catheterization of the left profunda femoris artery corroborates the CT angiographic finding of high-grade profunda femoris artery (*P*) stenosis (arrows). **(f)** DSA image of left superficial femoral artery shows multiple focal stenoses (arrowheads) in the same segment of the superficial femoral artery as demonstrated by CT angiography. Note the lack of calcium visualization on the subtracted image from DSA. **(g)** DSA image of the calf confirms single peroneal vessel runoff. **(h)** DSA image of left foot confirms reconstitution of the dorsalis pedis artery (*DP*) from the peroneal artery (arrowheads).

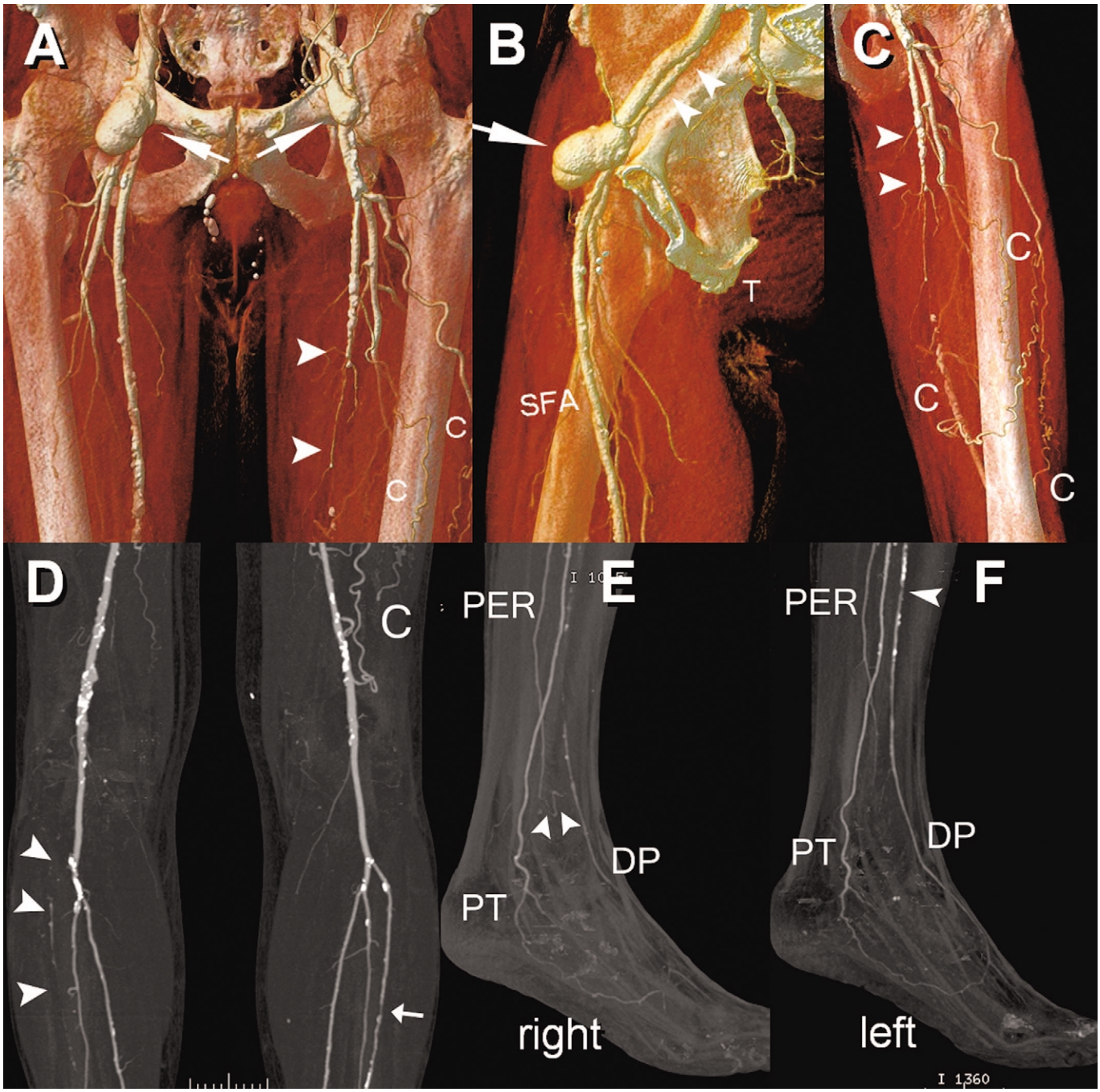

Figure 11. Perianastomotic pseudoaneurysms with bilateral infrainguinal disease in an 87-year-old man with claudication and history of aortobifemoral bypass grafting. **(a)** VR image demonstrates bilateral perianastomotic pseudoaneurysms at the distal attachment sites of the aortobifemoral graft and common femoral arteries (arrows). There is a long-segment superficial femoral artery occlusion on the left (arrowheads) with collateral vessels from the profunda femoris artery (*c*). **(b)** Thick-slab VR image of the right groin (left lateral view) shows the profile of the pseudoaneurysm (arrow), as well as the adjacent native external iliac artery (arrowheads). The proximal and mid-right superficial femoral artery is patent (*SFA*). *T*, ischial tuberosity. **(c)** VR image of the left thigh demonstrates abundant profunda collateral supply (*c*), which reconstitutes the distal superficial femoral artery. The length of the occluded segment was approximately 11 cm (arrowheads). **(d)** MIP of both knees shows occlusion of the right anterior tibial artery at its origin (arrowheads). There is a focal significant stenosis in the midportion of the left anterior tibial artery (arrow). Heavy popliteal artery calcific plaque is present bilaterally. **(e,f)** MIP of both feet with bone segmentation demonstrates patent posterior tibial arteries (*PT*) at both ankles into the feet. Peroneal arteries (*PER*) are patent to the lower calves. **(e)** There is reconstitution of the right dorsalis pedis (*DP*) via peroneal collaterals (arrowheads). The left dorsalis pedis is patent. **(f)** The focal left anterior tibial stenosis is again identified (arrowhead).

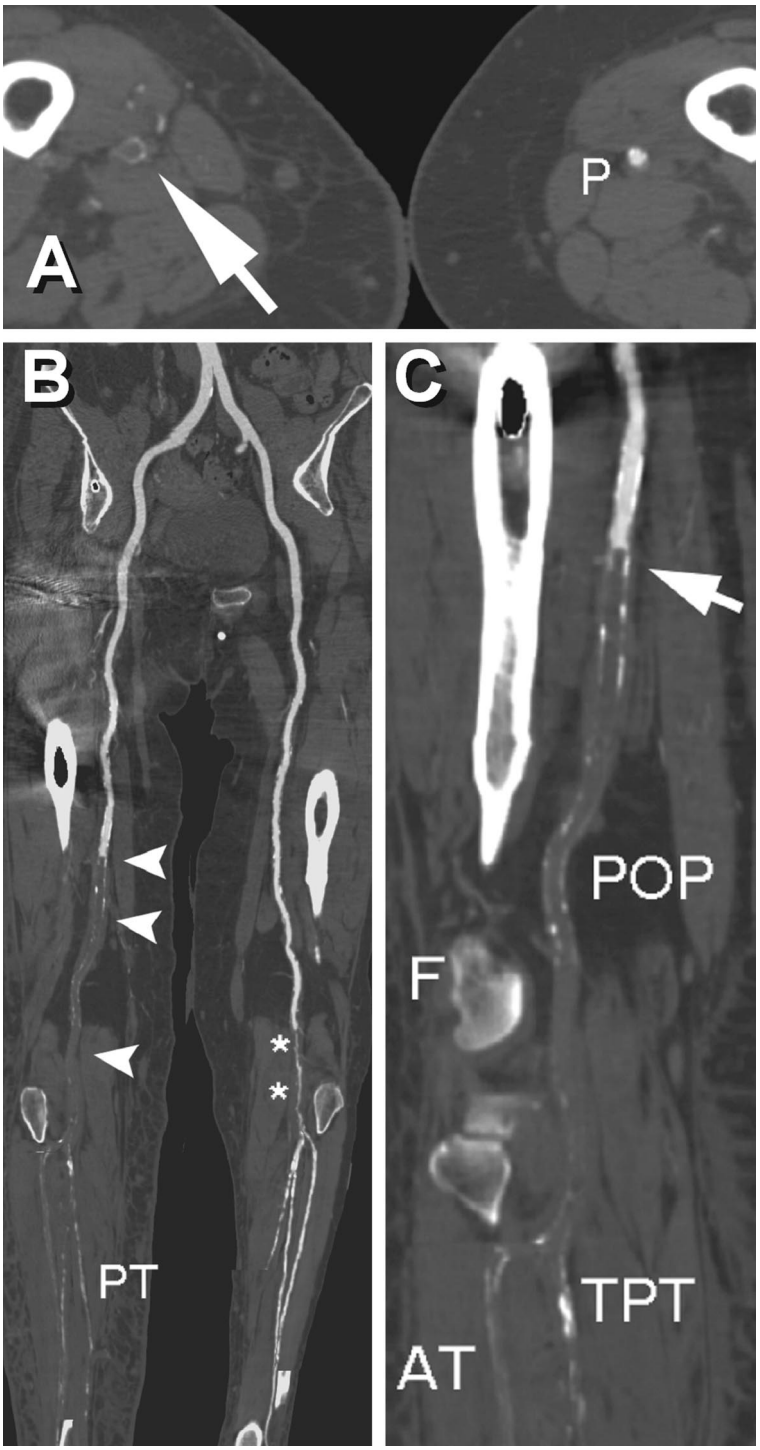

Figure 12. Acute thrombosis of the femoropopliteal and trifurcation vessels in an 84-year-old woman with an acutely cool right leg. The patient refused angiography. **(a)** Transverse CT angiographic image at the level of the adductor canal shows rounded filling defect in the right popliteal artery (arrow). The contralateral left popliteal artery (*P*) is patent at this level. **(b)** Large field of view multipath CPR and **(c)** enlarged image of popliteal region show the extent of right-sided thrombus (arrowheads). In addition to the popliteal artery (*POP*), the anterior tibial artery (*AT*), tibioperoneal trunk (*TPT*), and posterior tibial artery (*PT*) are occluded. *F*, femoral condyle. High-grade left popliteal stenosis (asterisk) is also noted.

raphy (DSA; **Table 5**) (8–11). In general, sensitivity and specificity are greater for arterial occlusions than for the detection of stenoses. Accuracy and interobserver agreement are also greater for femoropopliteal and iliac vessels compared with infrapopliteal arteries when four-channel CT is used. In the first study of submillimter collimated 16-channel CT (30), the overall sensitivities, specificities, and accuracies were all greater than 96% and there was no evident decrease of performance down to the popliteocrural branches. Pedal arteries have not been specifically analyzed in any published series to our knowledge. The presence of vessel calcifications apparently reduces diagnostic performance of multiple–detector row CT in general.

Ouwendijk and coworkers (31) recently evaluated the clinical utility, patient outcomes and costs of peripheral MR angiography and 16-channel CT angiography for initial imaging and diagnostic workup of 157 patients with peripheral arterial disease. In this randomized prospective study, confidence was slightly greater with CT and patients in the CT group underwent less additional imaging studies and had greater improvement of clinical outcomes after treatment, but none of these differences were statistically significant. However, average diagnostic imaging costs were significantly lower with CT compared with MR angiography.

CURRENT CLINICAL APPLICATIONS

CT angiography is increasingly used at many institutions, such as our own, for imaging the lower-extremity vasculature over a wide range of clinical indications. Evaluation of atherosclerotic steno-occlusive disease and its complications is the main application of CT angiography at our institution. However, congenital abnormalities, traumatic and iatrogenic injuries, inflammatory conditions, drug toxicity, embolic phenomena, and aneurysmal changes can also affect the arteries of the lower extremities. CT angiography may be used in many of these conditions.

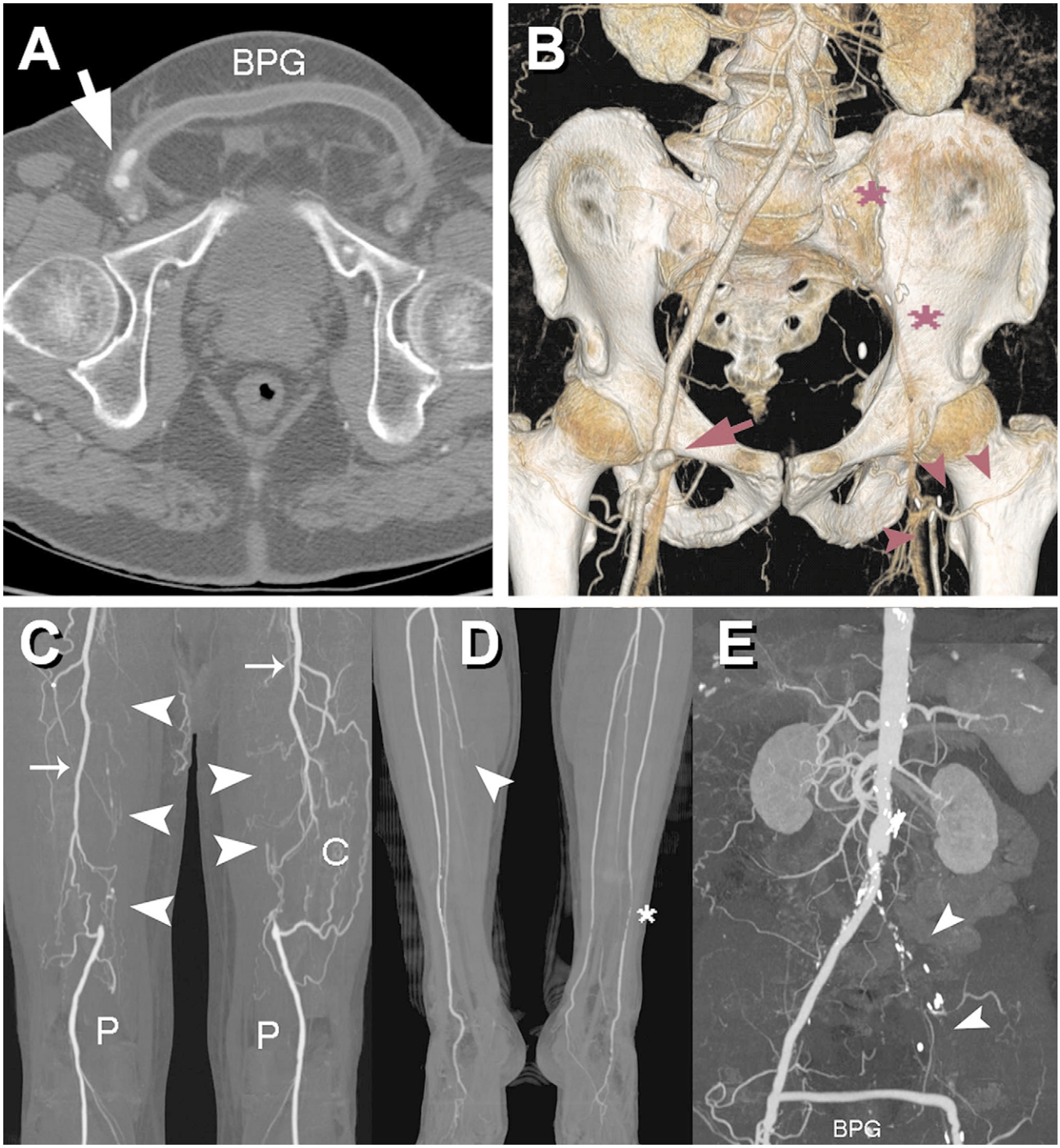

Figure 13. Utility of peripheral CT angiography in monitoring bypass graft patency in a 74-year-old man with a surgically placed femorofemoral bypass graft for chronic left iliac arterial occlusion. The patient presented with rest pain after recent surgical bypass procedure. Pain and bandages prevented adequate Doppler imaging and physical examination. **(a)** Axial CT angiography shows lack of contrast material opacification of the femorofemoral bypass graft (*BPG*). Only the right common femoral artery is patent (arrow). **(b)** Volume-rendered image demonstrates only a short area of flow at the right bypass graft anastomosis (arrow). There is complete occlusion of the left iliac arterial system (asterisks) and reconstitution of the left profunda femoris artery by collateral vessels to the lateral femoral circumflex artery (arrowheads). **(c)** MIP image at the level of the thighs shows bilateral long-segment superficial femoral artery occlusions (arrowheads), with reconstitution of the popliteal arteries (*P*) via collateral vessels (*C*) from the profunda femoris arteries (arrows). **(d)** MIP image of calf arteries demonstrates three-vessel runoff in the left lower extremity. There is occlusion of the right posterior tibial artery (arrowhead) in the mid-calf. Segmentation artifact from automated bone removal is noted (asterisk). **(e)** MIP image of the abdomen and bilateral groin region 3 days later demonstrates interval surgical revision of femorofemoral bypass graft (*BPG*), with restored patency. Left iliac occlusion is again noted (arrowheads).

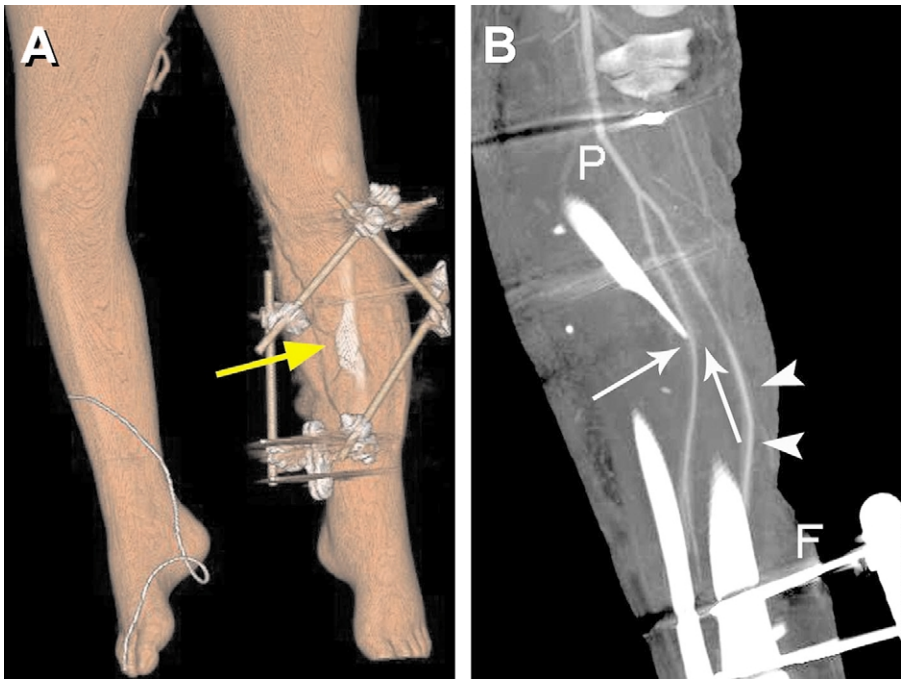

Figure 14. Utility of peripheral CT angiography for preoperative vascular mapping in a 24-year-old woman after a motor vehicle accident with tibial/fibular fractures and degloving injury. Preoperative CT angiography was requested to evaluate patency and position of calf runoff vessels. **(a)** VR image with opacity transfer functions adjusted for skin detail. There is extensive soft-tissue injury including exposed bone (yellow arrow). An external fixator for tibial/fibular fracture is also noted. **(b)** Oblique MIP image of left calf shows bowing of the peroneal artery secondary to mass effect from adjacent displaced fibular fracture (white arrows). Popliteal (*P*) and posterior tibial arteries are patent (arrowheads). *F*, external fixator.

Intermittent Claudication

In patients with claudication, treatment aims at improving blood supply to the femoral and calf muscles, and is therefore usually limited to the aortoiliac and femoropopliteal vascular territories. Medical management including exercise regimens, tobacco cessation programs, and drug therapy may improve symptoms (32–34), but patient compliance is often poor. Surgical or endovascular revascularization is then considered. For many patients, angioplasty is more cost-effective than surgical intervention (35). The original American Heart Association task force guidelines (36) and the TransAtlantic Inter-Society Consensus report (37) have provided guidelines for appropriate treatment of femoropopliteal disease. Conventional treatment of aortoiliac lesions and short (<5 cm) femoropopliteal stenoses or occlusions (TransAtlantic Inter-Society Consensus A or B) typically has been endovascular, whereas longer femoral occlusions (TransAtlantic Inter-Society Consensus C or D) and occlusions involving the common femoral artery may require surgical revascularization. Factors influencing the method of treatment depend on the lesion's morphology (degree of stenosis/occlusion and lesion length) (38) and location, and most importantly, the status of runoff vessels. The STAR Registry report and others have shown distal runoff vessel patency (and diabetes) as the most important lesion characteristic with regard to expected long-term patency (39). Additional improvements in catheter and guide wire design and techniques such as subintimal recanalization (40–43) have expanded the range of lesions that can be adequately treated percutaneously. The calf arteries are not a primary target for endovascular or surgical treatment in patients with claudication, but are important as a predictor of short- and long-term patency rates after femoropopliteal intervention.

CT angiography can provide complete delineation of the femoropopliteal segment and inflow and outflow arteries, including lesion number, lengths, stenosis diameter and morphology, adjacent normal arterial caliber, degree of calcification, and status of distal runoff vessels (**Fig 10**). These factors allow precise preprocedural planning with regard to route of access (**Figs 8–10**), balloon selection, and expected long-term patency after intervention. Effects of eccentric stenoses on luminal diameter reduction are also well-defined by multiple–detector row CT angiography, ie, a more accurate determination of diameter reduction may be possible with multiple–detector row CT angiography versus DSA alone (44). Status of collateral vessels is well-assessed on MIP and VR images, and arterial segments distal to long-segment occlusions are well-visualized (**Fig 11**). From a financial perspective, preprocedural US or MR angiography has been shown to be cost-effective relative to catheter angiography (45); it is expected that CT angiography is also cost-effective in this regard (45,46).

Chronic Limb-threatening Ischemia

Patients with chronic limb-threatening ischemia also benefit from treatment of aortoiliac and femoropopliteal lesions, which are the initial target for intervention if present. Because the treatment goal in this patient group is the prevention of tissue loss and need for amputation, assessment and promotion of blood flow through the calf arteries is of much greater importance than in patients with intermittent claudication. A variety of endovascular techniques have shown efficacy in the treatment of infrapopliteal lesions (47,48). Creation of a road map to lesions amenable to angioplasty or other endovascular techniques and delineation of patent, acceptable target vessels for distal bypass are the challenges of vessel analysis in this advanced disease setting. Use of very thin collimation (≤1 mm) and optimization of contrast medium administration will provide improved visualization of these small vessels. The newest generation of 64-channel CT machines

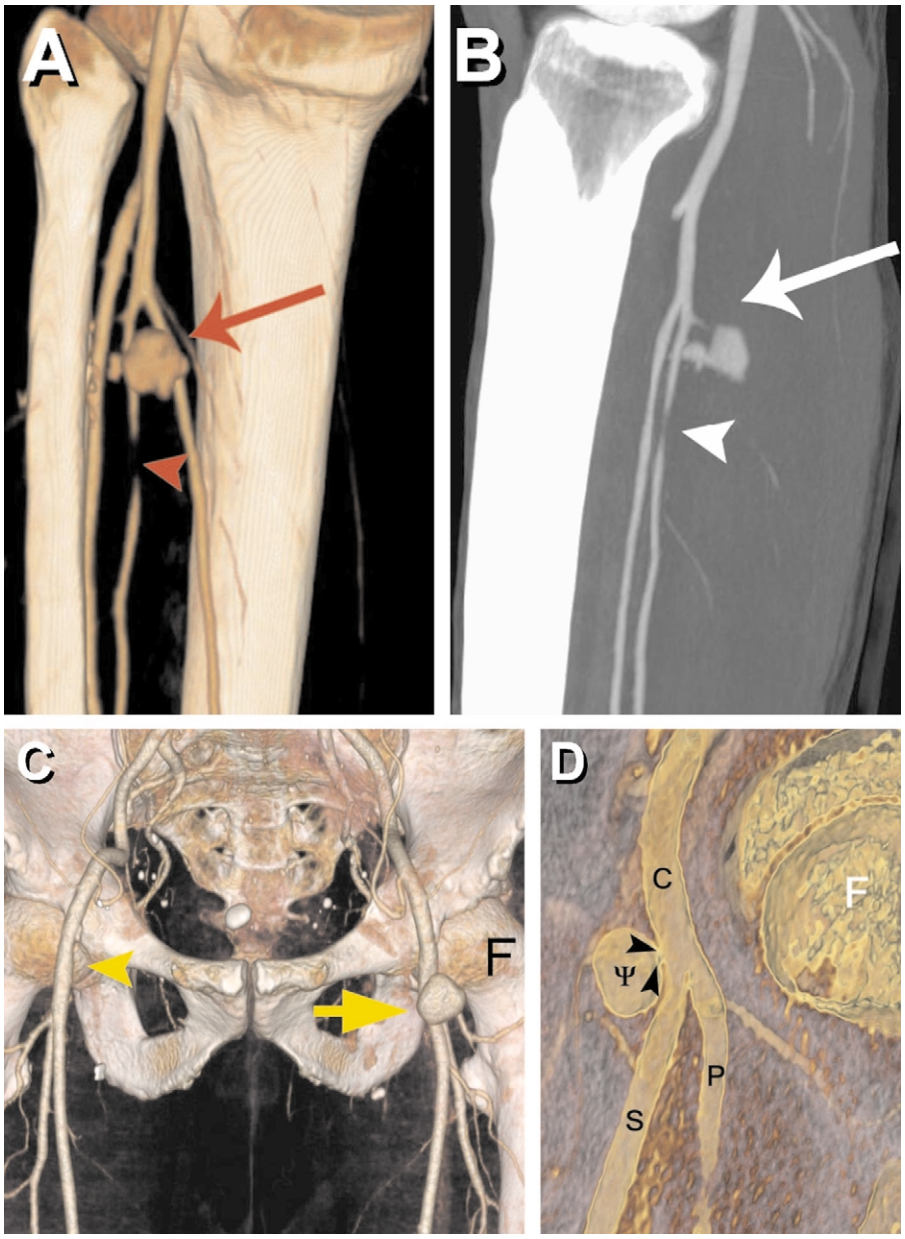

Figure 15. **(a,b)** Peripheral CT angiography of penetrating trauma in a 16-year-old male patient with a gunshot wound to the left leg. **(a)** Posterior VR image and **(b)** oblique thin-slab MIP image of the left calf show a lobulated pseudoaneurysm arising from the peroneal artery (arrow). The immediate distal peroneal artery shows luminal narrowing, most likely spasm (arrowhead). The remainder of the trifurcation vessels and adjacent bony structures are intact. **(c,d)** Images in a 45-year-old man with groin hematoma after cardiac catheterization. **(c)** VR image of the pelvis shows a rounded mass at the left common femoral bifurcation (arrow), consistent with pseudoaneurysm. The contralateral right common femoral artery is normal (arrowhead). *F*, femoral head. **(d)** Sagittal thin-slab VR image with opacity transfer function set to render translucent vessel interior demonstrates a narrow neck (arrowheads) of the pseudoaneurysm (Ψ), which arises from the common femoral artery (*c*) immediately proximal to the bifurcation of the superficial femoral artery (*S*) and profunda femoris artery (*P*). *F*, femoral head.

allows for further increase in spatial resolution and should allow improved visualization of small crural and pedal vessels. It is hoped these technical improvements translate to improved diagnostic accuracy and treatment planning; results from ongoing clinical studies are eagerly anticipated.

Aneurysms

Aneurysmal disease can affect any portion of the lower-extremity arterial system. Popliteal artery aneurysms are of particular interest as a source of distal embolic material and as a marker for the presence of abdominal aortic aneurysm. Peripheral CT angiography provides a rapid, noninvasive, cost-effective alternative to catheter angiography for detection and characterization of lower-extremity aneurysms. CT angiography yields robust data on aneurysm size, presence and amount of thrombus, presence of distal embolic disease, associated significant proximal and distal steno-occlusive disease, and detection of coexistent abdominal or iliac aneurysms (**Fig 6**). Three-dimensional volumetric analysis provides accurate measurement of aneurysm volume and luminal dimension.

Acute Ischemia

Few published data are available regarding the use of CT angiography in the setting of acute lower-extremity ischemia. If immediate percutaneous intervention (eg, thrombolysis) is planned, catheter angiography may be the most appropriate choice. If urgent surgical intervention is warranted based on the clinical status of the leg (ie, Rutherford criteria) (49), CT angiography may add an unnecessary delay to definitive therapy. CT angiography may be helpful in certain situations to guide the choice of percutaneous or surgical intervention and to aid in preprocedural planning. Determination of the extent and location of thrombosis can be accomplished by CT angiography. If thrombus or emboli involves all trifurcation vessels or a previously patent bypass graft or resides within a popliteal aneurysm, thrombolytic therapy may be most efficacious option (50). Demonstration of thrombus in locations not accessible to embolectomy could also direct therapy to catheter-based techniques. Large vessel thrombus or a recently thrombosed bypass graft could be best treated surgically (50). In the subacute ischemic setting, in which surgery may be best, CT angiography offers a complete overview of the affected vascular territories for optimum surgical

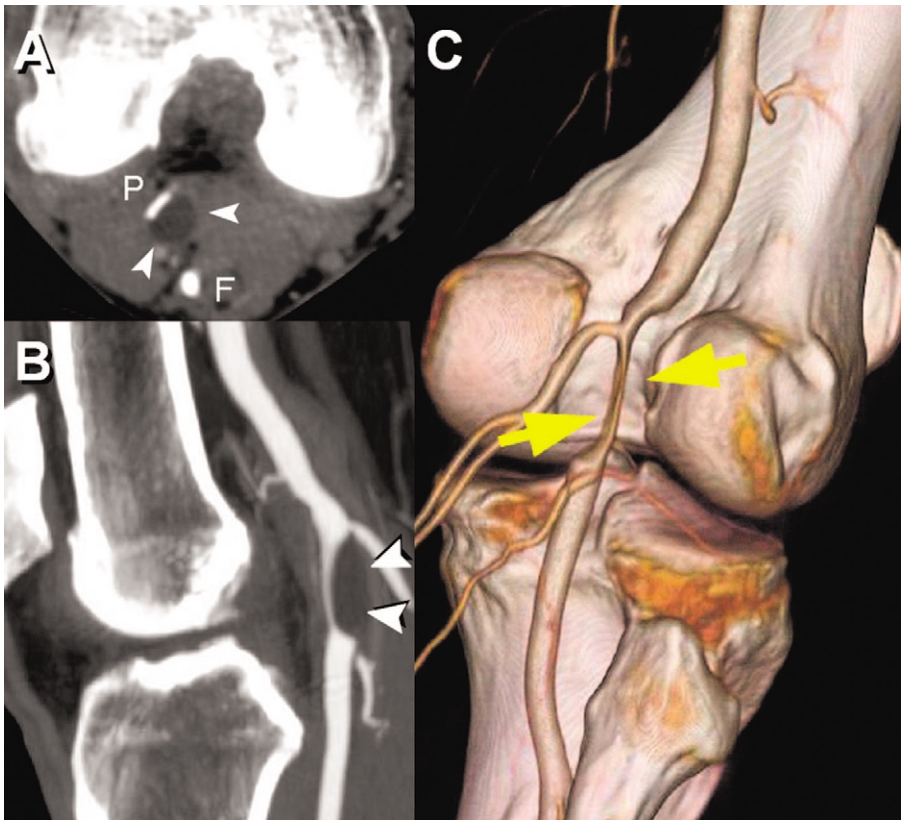

Figure 16. Images of adventitial cystic disease in a 55-year-old patient. **(a)** Axial source image from peripheral CT angiography shows marked compression of the popliteal artery (*P*) by an ovoid fluid-density lesion (arrowheads). Note the predominant transverse compression of the flow lumen. *F*, fabella. **(b)** Corresponding sagittal thin-slab MIP image shows craniocaudal extent of fluid-density lesion in the popliteal arterial wall (arrowheads). **(c)** VR image viewed obliquely from the posterior direction demonstrates severe narrowing of the right popliteal artery (arrows).

treatment. Patients who refuse catheter angiography and/or thrombolysis may also be rapidly and adequately evaluated by CT angiography (**Fig 12**). A delayed phase CT angiography acquisition initiated immediately after the initial arterial phase is often helpful to differentiate patent but slowly flowing vessels from thrombus.

Follow-up and Surveillance after Surgical or Percutaneous Revascularization

CT angiography is accurate and reliable in the assessment of peripheral arterial bypass grafts and detection of graft-related complications, including stenosis, aneurysmal changes, and arteriovenous fistulas (**Figs 11,13**). This is helpful in the immediate postoperative period, when US is limited by the presence of bandages and wounds (51). CT angiography can also demonstrate the results of percutaneous interventions, reveal residual disease, and diagnose vascular and extravascular complications.

CT angiography is not the first choice for routine bypass graft surveillance or for serial follow-up evaluation after intervention (eg, in research protocols) because US is easy to perform and reliable in this setting (52,53). However, CT is a very convenient problem-solving tool for the workup of patients with nondiagnostic US studies (limited access as a result of skin lesions, draping, or obesity), when US results are equivocal, or when ankle-brachial measurements and US yield conflicting results. In this setting, CT angiography has replaced catheter DSA completely at our institution and is used to decide further management.

Vascular Trauma

CT angiography, even with single–detector row CT, has been shown to be an accurate and useful test in the setting of suspected vascular trauma (5), and can replace diagnostic angiography. CT is easily accessible (often within or adjacent to the emergency department), and examination time is short. Moreover, CT angiography can be performed in combination with CT of other organ systems (eg, abdomen, chest) for complete delineation of the distribution and severity of injuries in each individual organ system (54). Traumatic arterial injuries and relationship of arterial segments to adjacent fractures and soft-tissue injuries are well-depicted (**Fig 14**). CT angiography reliably depicts hematoma and associated vascular compression or pseudoaneurysm, and can simultaneously show bone fragments. Bullets or other metal artifacts, if present, may limit small portions of the acquired volume.

Extremity CT angiography is also used for pediatric trauma patients (54). Particular attention to radiation dose and contrast medium is mandatory in this instance. Limited scan range, reduced dose settings, and a limit of 2 mL/kg body weight of contrast medium are employed to maximize patient safety.

Visualization is straightforward. For initial diagnosis, transverse images are usually sufficient, although MPR image creation and viewing may improve rapidity of analysis (**Fig 15**). The addition of VR images improves depiction of the anatomic relationship between arteries and adjacent bony/soft tissue injuries and foreign bodies. Generation of real-time 3D and/or VR images also promotes rapid communication to, and understanding by, referring clinical services.

Vascular Mapping

Data obtained from peripheral CT angiography in the setting of trauma are also of use when subsequent surgical reconstruction is performed (**Fig 14**). Additionally, precise knowledge of arterial anatomy is paramount when plastic surgical reconstruction for various diseases is considered. Fibular free flap procurement requires preoperative assessment of the limb to

prevent ischemic complications and failure of the flap and to exclude variant peroneal artery anatomy and occlusive disease, which could alter the surgical procedure (55). Previously, catheter angiography, with its attendant costs and risks, was required for this assessment. CT angiography allows high-resolution 3D evaluation of arteries, veins, and soft tissues (56–58) with less risk and at lower cost than catheter angiography (56). Other potential uses for CT angiography include evaluation of character and vascular supply of musculoskeletal tumors (54) and evaluation of suitability of the thoracodorsal and internal mammary arteries before transverse rectus abdominis muscle flap reconstruction.

Other Indications

Multiple–detector row CT angiography can provide exquisite noninvasive characterization of many other vascular conditions affecting the lower extremity. Vascular malformations, arterial compression by adjacent masses, adventitial cystic disease (**Fig 16**), and popliteal entrapment syndrome (59) can be fully evaluated. In the latter case, image acquisition at rest and with provocative maneuvers (eg, active plantar flexion against resistance) allows determination of the anatomy of the medial head of the gastrocnemius and the dynamic degree of arterial obstruction. Vasculitides and inflammatory processes affecting adjacent vessels can be well-characterized and the relationship of soft tissue and bone infection to the arterial structures can be delineated (54).

SUMMARY

Peripheral CT angiography has excellent spatial resolution and can show exquisite detail of peripheral vasculature. The current generation of 16- to 64–detector-row CT scanners and the development of refined 3D rendering techniques have made peripheral CT angiography a powerful tool for noninvasive imaging and treatment planning of peripheral arterial disease.

References

1. Lawrence JA, Kim D, Kent KC, et al. Lower extremity spiral CT angiography versus catheter angiography. Radiology 1995; 194:903–908.
2. Rieker O, Duber C, Schmiedt W, et al. Prospective comparison of CT angiography of the legs with intraarterial digital subtraction angiography. AJR Am J Roentgenol 1996; 166:269–276.
3. Beregi JP, Elkohen M, Deklunder G, et al. Helical CT angiography compared with arteriography in the detection of renal artery stenosis. AJR Am J Roentgenol 1996; 167:495–501.
4. Kramer SC, Gorich J, Aschoff AJ, et al. Diagnostic value of spiral-CT angiography in comparison with digital subtraction angiography before and after peripheral vascular intervention. Angiology 1998; 49:599–606.
5. Soto JA, Munera F, Morales C, et al. Focal arterial injuries of the proximal extremities: helical CT arteriography as the initial method of diagnosis. Radiology 2001; 218:188–194.
6. Rubin GD, Schmidt AJ, Logan LJ, et al. Multidetector-row CT angiography of lower extremity occlusive disease: a new application for CT scanning. Radiology 1999; 210:588.
7. Rubin GD, Schmidt AJ, Logan LJ, et al. Multi-detector row CT angiography of lower extremity arterial inflow and runoff: initial experience. Radiology 2001; 221:146–158.
8. Ofer A, Nitecki SS, Linn S, et al. Multidetector CT angiography of peripheral vascular disease: a prospective comparison with intraarterial digital subtraction angiography. AJR Am J Roentgenol 2003; 180:719–724.
9. Martin ML, Tay KH, Flak B, et al. Multidetector CT angiography of the aortoiliac system and lower extremities: a prospective comparison with digital subtraction angiography. AJR Am J Roentgenol 2003; 180:1085–1091.
10. Ota H, Takase K, Igarashi K, et al. MDCT compared with digital subtraction angiography for assessment of lower extremity arterial occlusive disease: importance of reviewing cross-sectional images. AJR Am J Roentgenol 2004; 182:201–209.
11. Catalano C, Fraioli F, Laghi A, et al. Infrarenal aortic and lower-extremity arterial disease: diagnostic performance of multi-detector row CT angiography. Radiology 2004; 231: 555–563.
12. Fleischmann D, Rubin GD, Paik DS, et al. Stair-step artifacts with single versus multiple detector-row helical CT. Radiology 2000; 216:185–196.
13. Hartnell GG. Contrast angiography and MR angiography: still not optimum. J Vasc Interv Radiol 1999; 10:99–100.
14. Fleischmann D. Use of high-concentration contrast media in multiple-detector-row CT: principles and rationale. Eur Radiol 2003; 13(suppl 5): M14–M20.
15. Fleischmann D, Hittmair K. Mathematical analysis of arterial enhancement and optimization of bolus geometry for CT angiography using the discrete Fourier transform. J Comput Assist Tomogr 1999; 23:474–484.
16. Fleischmann D, Rubin GD, Bankier AA, et al. Improved uniformity of aortic enhancement with customized contrast medium injection protocols at CT angiography. Radiology 2000; 214: 363–371.
17. Bron KM. Femoral arteriography. In: Abrams HL, ed. Abrams angiography: vascular and interventional radiology, 3rd ed. Boston: LittleBrown, 1983:1835–1875.
18. Versteylen RJ, Lampmann LE. Knee time in femoral arteriography. AJR Am J Roentgenol 1989; 152:203.
19. Fleischmann D, Rubin GD. Quantification of intravenously administered contrast medium transit through the peripheral arteries: implications for CT angiography. Radiology 2005; 236: 1076–1082.
20. Portugaller HR, Schoellnast H, Hausegger KA, et al. Multislice spiral CT angiography in peripheral arterial occlusive disease: a valuable tool in detecting significant arterial lumen narrowing? Eur Radiol 2004; 14:1681–1687.
21. Qanadli SD, Chiappori V, Kelekis A, et al. Multislice computed tomography of peripheral arterial disease: New approach to optimize vascular opacification with 16-row platform. Eur Radiol 2004; 14 Suppl. 2:S304.
22. Milne EN. The significance of early venous filling during femoral arteriography. Radiology 1967; 88:513–8.
23. Koechl A, Kanitsar A, Lomoschitz E, et al. Comprehensive assessment of peripheral arteries using multi-path curved planar reformation of CTA datasets. Eur Radiol 2003; 13:268–269.
24. Kanitsar A, Fleischmann D, Wegenkittl R, et al. CPR—curved planar reformation. In: IEEE Visualization. Boston: IEEE Computer Society; 2002;37–44.
25. Raman R, Napel S, Beaulieu CF, et al. Automated generation of curved planar reformations from volume data: method and evaluation. Radiology 2002; 223:275–280.
26. Fleischmann D, Kanitsar A, Lomoschitz E, et al. Multi-path curved planar reformation of the peripheral arterial tree. Radiology 2002; 225:363.
27. Napel S, Rubin GD, Jeffrey RB Jr. STS-MIP: a new reconstruction technique for CT of the chest. J Comput Assist Tomogr 1993; 17:832–838.
28. Raman R, Napel S, Rubin GD. Curved-slab maximum intensity pro-

jection: method and evaluation. Radiology 2003; 229:255–260.
29. Edwards AJ, Wells IP, Roobottom CA. Multidetector row CT angiography of the lower limb arteries: a prospective comparison of volume-rendered techniques and intra-arterial digital subtraction angiography. Clin Radiol 2005; 60:85–95.
30. Willmann JK, Baumert B, Schertler T, et al. Aortoiliac and lower extremity arteries assessed with 16-detector row CT angiography: prospective comparison with digital subtraction angiography. Radiology 2005; 236:1083–1093.
31. Ouwendijk R, de Vries M, Pattynama PM, et al. Imaging peripheral arterial disease: a randomized controlled trial comparing contrast-enhanced MR angiography and multi-detector row CT angiography. Radiology 2005; 236: 1094–1103.
32. Hiatt WR. Medical treatment of peripheral arterial disease and claudication. N Engl J Med 2001; 344:1608–1621.
33. Hiatt WR. Pharmacologic therapy for peripheral arterial disease and claudication. J Vasc Surg 2002; 36:1283–1291.
34. Stewart KJ, Hiatt WR, Regensteiner JG, et al. Exercise training for claudication. N Engl J Med 2002; 347:1941–1951.
35. de Vries SO, Visser K, de Vries JA, et al. Intermittent claudication: cost-effectiveness of revascularization versus exercise therapy. Radiology 2002; 222:25–36.
36. Pentecost MJ, Criqui MH, Dorros G, et al. Guidelines for peripheral percutaneous transluminal angioplasty of the abdominal aorta and lower extremity vessels. A statement for health professionals from a special writing group of the Councils on Cardiovascular Radiology, Arteriosclerosis, Cardio-Thoracic and Vascular Surgery, Clinical Cardiology, and Epidemiology and Prevention, the American Heart Association. Circulation 1994; 89:511–531.
37. Dormandy JA, Rutherford RB. Management of peripheral arterial disease (PAD). TASC Working Group. TransAtlantic Inter-Society Consensus (TASC). J Vasc Surg 2000; 31(suppl): S1–S296.
38. Surowiec SM, Davies MG, Eberly SW, et al. Percutaneous angioplasty and stenting of the superficial femoral artery. J Vasc Surg 2005; 41:269–278.
39. Clark TW, Groffsky JL, Soulen MC. Predictors of long-term patency after femoropopliteal angioplasty: results from the STAR registry. J Vasc Interv Radiol 2001; 12:923–933.
40. Reekers JA, Bolia A. Percutaneous intentional extraluminal (subintimal) recanalization: how to do it yourself. Eur J Radiol 1998; 28:192–198.
41. Tisi PV, Mirnezami A, Baker S, et al. Role of subintimal angioplasty in the treatment of chronic lower limb ischaemia. Eur J Vasc Endovasc Surg 2002; 24:417–422.
42. Saketkhoo RR, Razavi MK, Padidar A, et al. Percutaneous bypass: subintimal recanalization of peripheral occlusive disease with IVUS guided luminal re-entry. Tech Vasc Interv Radiol 2004; 7:23–27.
43. Nadal LL, Cynamon J, Lipsitz EC, et al. Subintimal angioplasty for chronic arterial occlusions. Tech Vasc Interv Radiol 2004; 7:16–22.
44. Hirai T, Korogi Y, Ono K, et al. Maximum stenosis of extracranial internal carotid artery: effect of luminal morphology on stenosis measurement by using CT angiography and conventional DSA. Radiology 2001; 221:802–809.
45. Visser K, de Vries SO, Kitslaar PJ, et al. Cost-effectiveness of diagnostic imaging work-up and treatment for patients with intermittent claudication in The Netherlands. Eur J Vasc Endovasc Surg 2003; 25:213–223.
46. Rubin GD, Armerding MD, Dake MD, et al. Cost identification of abdominal aortic aneurysm imaging by using time and motion analyses. Radiology 2000; 215:63–70.
47. Clair DG, Dayal R, Faries PL, et al. Tibial angioplasty as an alternative strategy in patients with limb-threatening ischemia. Ann Vasc Surg 2005; 19: 63–68.
48. Dorros G, Jaff MR, Murphy KJ, et al. The acute outcome of tibioperoneal vessel angioplasty in 417 cases with claudication and critical limb ischemia. Cathet Cardiovasc Diagn 1998; 45:251–256.
49. Rutherford RB, Baker JD, Ernst C, et al. Recommended standards for reports dealing with lower extremity ischemia: revised version. J Vasc Surg 1997; 26: 517–538.
50. Costantini V, Lenti M. Treatment of acute occlusion of peripheral arteries. Thromb Res 2002; 106:V285–V294.
51. Willmann JK, Mayer D, Banyai M, et al. Evaluation of peripheral arterial bypass grafts with multi-detector row CT angiography: comparison with duplex US and digital subtraction angiography. Radiology 2003; 229:465–474.
52. Mills JL, Harris EJ, Taylor LM Jr, et al. The importance of routine surveillance of distal bypass grafts with duplex scanning: a study of 379 reversed vein grafts. J Vasc Surg 1990; 12:379–386.
53. Moody P, Gould DA, Harris PL. Vein graft surveillance improves patency in femoro-popliteal bypass. Eur J Vasc Surg 1990; 4:117–21.
54. Karcaaltincaba M, Akata D, Aydingoz U, et al. Three-dimensional MDCT angiography of the extremities: clinical applications with emphasis on musculoskeletal uses. AJR Am J Roentgenol 2004; 183:113–117.
55. Whitley SP, Sandhu S, Cardozo A. Preoperative vascular assessment of the lower limb for harvest of a fibular flap: the views of vascular surgeons in the United Kingdom. Br J Oral Maxillofac Surg 2004; 42:307–310.
56. Klein MB, Karanas YL, Chow LC, et al. Early experience with computed tomographic angiography in microsurgical reconstruction. Plast Reconstr Surg 2003; 112:498–503.
57. Karanas YL, Antony A, Rubin G, et al. Preoperative CT angiography for free fibula transfer. Microsurgery 2004; 24: 125–127.
58. Chow LC, Napoli A, Klein MB, et al. Vascular mapping of the leg with multi-detector row CT angiography prior to free-flap transplantation. Radiology 2005; 237:353–360.
59. Takase K, Imakita S, Kuribayashi S, et al. Popliteal artery entrapment syndrome: aberrant origin of gastrocnemius muscle shown by 3D CT. J Comput Assist Tomogr 1997; 21:523–528.